Journal Pre-proof

Amphiphilic Desmuramyl Peptides for the Rational Design of New Vaccine Adjuvants: Synthesis, *In Vitro* Modulation of Inflammatory Response and Molecular Docking Studies

Farooq-Ahmad Khan, Nourina Nasim, Yan Wang, Alaa Alhazmi, Mehar Sanam, Zaheer Ul-Haq, Damayanthi Yalamati, Marina Ulanova, Zi-Hua Jiang

PII: S0223-5234(20)30835-7

DOI: https://doi.org/10.1016/j.ejmech.2020.112863

Reference: EJMECH 112863

To appear in: *European Journal of Medicinal Chemistry*

Received Date: 30 June 2020

Revised Date: 14 September 2020

Accepted Date: 16 September 2020

Please cite this article as: F.-A. Khan, N. Nasim, Y. Wang, A. Alhazmi, M. Sanam, Z. Ul-Haq, D. Yalamati, M. Ulanova, Z.-H. Jiang, Amphiphilic Desmuramyl Peptides for the Rational Design of New Vaccine Adjuvants: Synthesis, *In Vitro* Modulation of Inflammatory Response and Molecular Docking Studies, *European Journal of Medicinal Chemistry*, https://doi.org/10.1016/j.ejmech.2020.112863.

Amphiphilic Desmuramyl Peptides for the Rational Design of New Vaccine Adjuvants: Synthesis, *In Vitro* Modulation of Inflammatory Response and Molecular Docking Studies

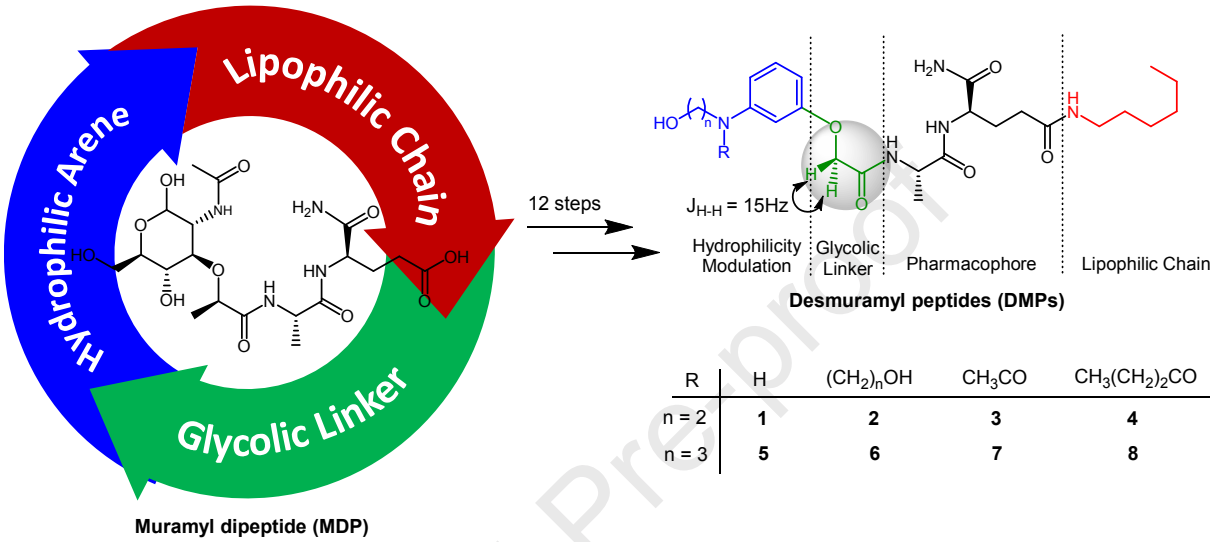

R	H	$(CH_2)_nOH$	CH_3CO	$CH_3(CH_2)_2CO$
n = 2	**1**	**2**	**3**	**4**
n = 3	**5**	**6**	**7**	**8**

Amphiphilic Desmuramyl Peptides for the Rational Design of New Vaccine Adjuvants: Synthesis, *In Vitro* Modulation of Inflammatory Response and Molecular Docking Studies

Farooq-Ahmad Khan[a, f *], Nourina Nasim[a], Yan Wang[a], Alaa Alhazmi[b,c], Mehar Sanam[a], Zaheer Ul-Haq[d], Damayanthi Yalamati[e], Marina Ulanova[b], Zi-Hua Jiang[f *]

[a] H.E.J. Research Institute of Chemistry, International Center for Chemical & Biological Sciences, University of Karachi-75270, Pakistan.

[b] Medical Sciences Division, Northern Ontario School of Medicine, Lakehead University, 955 Oliver Road, Thunder Bay, Ontario, P7B 5E1, Canada.

[c] Medical Laboratory Technology Department, Jazan University, Jazan, Saudi Arabia.

[d] Dr. Panjwani Center for Molecular Medicine and Drug Research, International Center for Chemical and Biological Sciences, University of Karachi, Karachi-75270, Pakistan.

[e] Alberta Research Chemicals Inc., 11421 Saskatchewan Drive, Edmonton, Alberta, T6G 2M9, Canada.

[f] Department of Chemistry, Lakehead University, 955 Oliver Road, Thunder Bay, Ontario, P7B 5E1, Canada.

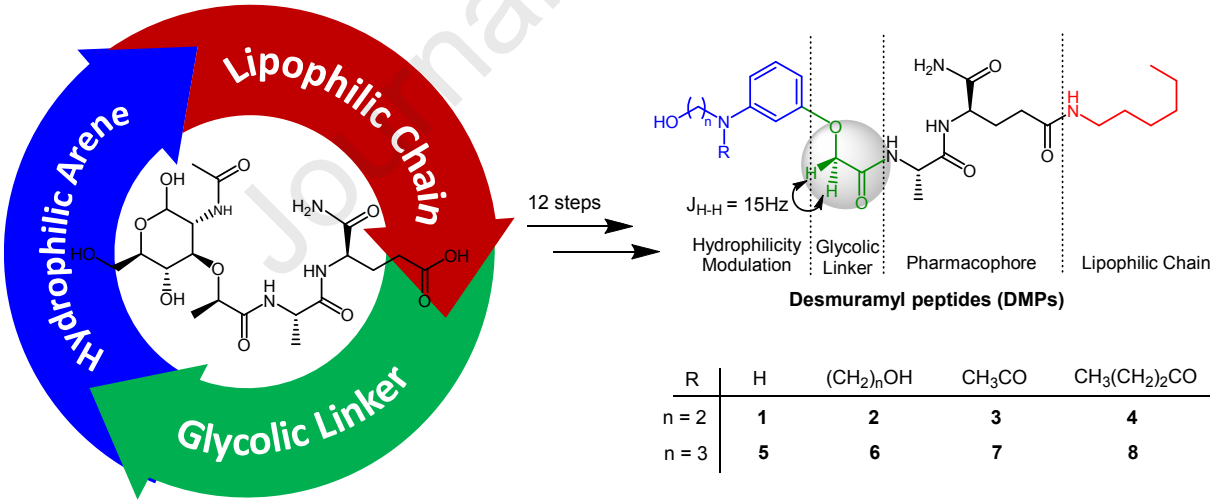

R	H	$(CH_2)_nOH$	CH_3CO	$CH_3(CH_2)_2CO$
n = 2	**1**	**2**	**3**	**4**
n = 3	**5**	**6**	**7**	**8**

---

* Corresponding authors

Tel: +92 111 222 292; fax: +92 21 348 19018-9; email: farooq.khan@iccs.edu
Tel: +1 807 766 7171; fax: +1 807 346 7775; email: zjiang@lakeheadu.ca

Highlights

1. New type of desmuramyl peptides having hydrophilic aryl scaffolds were synthesized.
2. Their preparation involves an efficient 12 step synthesis strategy.
3. They can effectively modulate the inflammatory response of THP-1 cells.
4. High levels of TNF-α – a major proinflammatory cytokine – were released.
5. Molecular docking studies indicate strong binding to NOD2 receptor.

Key Words

Desmuramyl peptides, ICAM-1, Immunomodulatory agents, TNF-α, NOD2 ligands.

Abstract

Nucleotide-binding oligomerization domain 2 (NOD2) is cytosolic surveillance receptor of the innate immune system capable of recognizing the bacterial and viral infections. Muramyl dipeptide (MDP) is the minimal immunoreactive unit of murein. NOD2 perceives MDP as pathogen-associated molecular pattern, thereby triggering an immune response with undesirable side-effects. Beneficial properties of MDP, such as pro-inflammatory characteristics for the rational design of new vaccine adjuvants, can be harnessed by strategically re-designing the molecule. In this work, a new class of amphiphilic desmuramylpeptides (DMPs) were synthesized by replacing the carbohydrate moiety (muramic acid) of the parent molecule with hydrophilic arenes. A lipophilic chain was also introduced at the *C*-terminus of dipeptide moiety (alanine-isoglutamine), while conserving its L-D configuration. These novel DMPs were found to set off the release of higher levels of tumour necrosis factor alpha (TNF-α) than Murabutide, which is a well-known NOD2 agonist. Molecular docking studies indicate that all these DMPs bind well to NOD2 receptor with similar dock scores (binding energy) through a number of hydrogen bonding and hydrophobic/π interactions with several crucial residues of the receptor. More studies are needed to further assess their immunomodulatory therapeutic potential, as well as the possible involvement of NOD2 activation.

1. Introduction

The innate immune system is the first-line of defense against pathogenic infections [1], which involves the evolutionary defense strategy via sentinel cells [2]. These cells are equipped with numerous pattern recognition receptors (PRRs), which provide surveillance by sensing the pathogen-associated molecular patterns (PAMPs) [3]. An anti-pathogen signaling cascade is

triggered upon PAMP detection, thereby alerting the immune system for an inflammatory response [4]. Bacterial peptidoglycan (PGN) and viral nucleic acids are common PAMP examples. Muramyl dipeptide (MDP) is the smallest PGN fragment recognized by our immune system via an intracellular NOD2 type PRR [5]. When MDP actuates NOD2, a downstream signaling pathway activates the NF-κB transcriptional factor that results in the release of pro-inflammatory cytokines, upregulation of adhesion molecules and nitric oxide (NO) secretion [6,7].

Muramyl dipeptide (MDP, Figure 1) was first discovered in the laboratory of E. Lederer at Université Paris-Sud in France [8]. It is composed of a dipeptide (L-alanine-D-isoglutamine) attached to a carbohydrate moiety (*N*-acetyl glucosamine) via lactic acid linker [9]. MDP is a potent immunostimulant due to its ability to induce the production of various pro-inflammatory cytokines [10]. Previous studies have shown that pre-exposure to MDP enhances the immune response to a later challenge [11]. Nevertheless, this molecule induces many undesirable pharmacological effects too, such as: endotoxic sensitization, induction of arthritis, bone resorption, transitory leukopenia and pyrogenicity [12]. Furthermore, poor cell membrane penetration and rapid elimination limit MDP application in clinical settings [13]. Interestingly, minor modification in the basic structure of MDP often leads to the separation of desirable biological activities from unwanted side effects [14]. Therefore, numerous structural variations of MDP have been performed to provide new chemical entities with improved therapeutic potential, which can stimulate the immune defense against infectious pathogens and express immunomodulatory activity without harmful side effects [11].

Many hydrophilic MDP derivatives have therefore been synthesized, leading to the discovery of several useful molecules, such as Murabutide and Muramethide (Figure 1).

Murabutide contains an aliphatic chain at the peptide end of hydrophilic MDP. This molecule was found to be non-pyrogenic and safe immunomodulator. It was also able to enhance the non-specific resistance against microbial infections without toxicity [15]. Besides, Nor-MDP and Temurtide also reached the clinical development stages. They lack pyrogenicity and interact safely with the immune system [16].

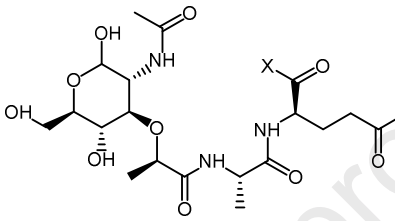

MDP: X = NH_2, Y = OH

Muramethide: X = OCH_3, Y = NH_2

Murabutide: X = $O(CH_2)_3CH_3$, Y = NH_2

Figure 1. Hydrosoluble MDP derivatives

Many lipophilic MDP analogs have also been developed by the pharmaceutical industry (Figure 2), such as Romurtide, Mifamurtide, and MTP-Cholesterol [17,18]. Interestingly, biological effects of some lipophilic derivatives extend far beyond their immunomodulatory properties. For example, MTP-PE (Mifamurtide) originally developed by Novartis, is now being used for osteosarcoma treatment [19].

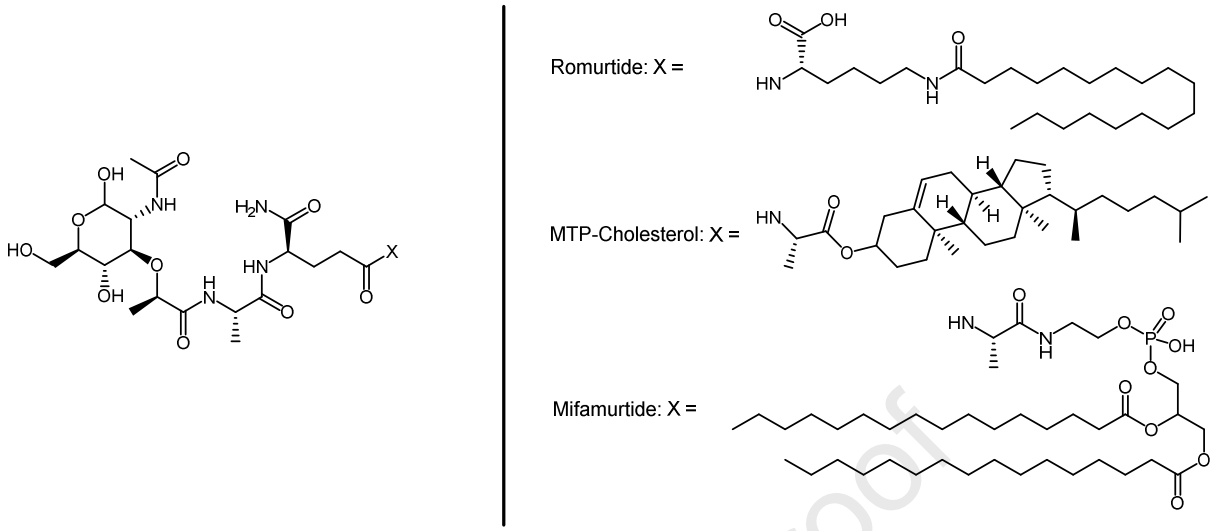

Figure 2. Lipophilic MDP derivatives developed by the pharmaceutical industry

In clinical settings, MTP-PE was shown to have immunomodulatory adjuvant properties in humans [20]. Its prophylactic antiviral activity was explored against Influenza [21], HIV [22,23] and Herpes Simplex [24] antigens. Other MDP derivatives, including the hydrosoluble ones, were also investigated as vaccine adjuvant for the induction of humoral and cellular immune response. Table 1 lists the selection of the derivatives used in experimental vaccines against human viruses. Overall results from the clinical trials suggest that the lipophilicity could potentially help these derivatives maintain their adjuvant activity while minimizing the pyrogenicity of parent MDP molecule.

Table 1. MDP derivatives used in Experimental Vaccines against Human Viruses

MDP Derivative	Vaccine / Virus Type
MTP-PE (Mifamurtide)	Influenza [21], HIV [22,23], Herpes Simplex [24]
Threonyl-MDP	Influenza [25], HIV [26], Hepatitis B [27]
GMDP	Influenza [28], HIV [29]
6-O-acyl MDP	Influenza [30,31], Hepatitis B [30]
Murabutide	Tetanus [32], Hepatitis B [33]

MDP analogs containing different carbohydrate moiety, such as galactose-, allose-, mannose-, furanose- and xylose-containing molecules were synthesized and evaluated too [34–37]. Only D-glucofuranose-containing MDP was reported to have better immunomodulatory activity than the parent MDP molecule [36]. The carbohydrate moiety in MDP is apparently not crucial for the immunomodulatory activity by this type of compounds [11]. Many MDP analogs lacking the carbohydrate fragment have shown some interesting immunomodulatory properties. These MDP analogs are commonly known as desmuramyl peptides (DMPs) in the literature [37–39]. One such example is O-(L-alanyl-D-isoglutamine-L-alanyl)-glycerol-3-mycolate which can stimulate the resistance to infection in mice, the results being comparable to the parent MDP [38]. Many DMPs have also shown significant antitumor potency with remarkable immunomodulatory properties [40]. Gang Liu and co-workers have done significant work in this regard [18,41–43]. In one instance, they replaced the carbohydrate moiety of MDP with hydrophobic arenes to afford paclitaxel (Taxol®) conjugated DMPs [42,44]. These conjugates combine the effects of immunotherapy and chemotherapy for the cancer treatment [44]. Numerous other DMPs incorporating various molecular scaffolds to replace the carbohydrate moiety have also been shown to display remarkable immunomodulatory activity [45–52] and promising antitumor effect [45,46].

Previously reported DMPs are mostly devoid of hydrophilic character due to the elimination of the carbohydrate fragment, and are lipophilic in nature. Lipophilicity is an important variable which helps eliminate several problems associated with this type of molecules, such as poor cell penetration and rapid elimination. Conversely, hydrophilicity is another important parameter for the activation of NOD2, which is located in the cytosolic aqueous environment. Additionally, the literature survey revealed that current protocols don't

mention the synthesis of desmuramyl peptides having lipophilic and hydrophilic characteristics simultaneously.

Owing to limited efficacy of traditional immunomodulatory agents, the development of non-toxic and multifunctional drugs having the ability to safely modify the immune response is of vital importance [50]. In the design of new amphiphilic DMPs (Figure 3) as potential vaccine adjuvants, we broke the molecule down to four fragments: 1) the dipeptide pharmacophore, 2) the hydrophilic aryl amine moiety replacing the carbohydrate, 3) the lipophilic chain at the C-terminus of the dipeptide, and 4) the linker between the aryl amine and the dipeptide. Firstly, MDP recognition by the immune system is highly stereospecific with respect to the configuration of the amino acid residues in the dipeptide moiety [10,53–55]. Conserving L-D configuration of dipeptide is therefore essential for the design of new MDP mimics [56]. Secondly, interesting biological activities can be obtained by adopting balanced hydrophilicity/lipophilicity of the molecule, with Murabutide (Figure 1) being a good example. The hydrophilicity of these DMPs could be modulated via hydroxylated *N*-alkyl group-containing aryl amine scaffold~~s~~ (Figure 3) to replace the carbohydrate moiety of MDP. Thirdly, a modest lipophilic chain was introduced at the *C*-terminus of the dipeptide moiety to adjust the lipophilicity of these DMPs and assist their penetration through the cell membrane and reach the cytosolic NOD2 receptor~~s~~. Fourthly, a glycolic acid linker was used in place of lactic acid to couple these hydrophilic aryl amines with the *N*-terminus of the dipeptide moiety, thereby eliminating the chirality of the linker and simplifying the structure of these DMPs. Although lactic acid chirality is known to influence the stability as well as activity of MDP, nor-MDP analogs lacking this chirality is reported to have comparable activity and lower toxicity [11].

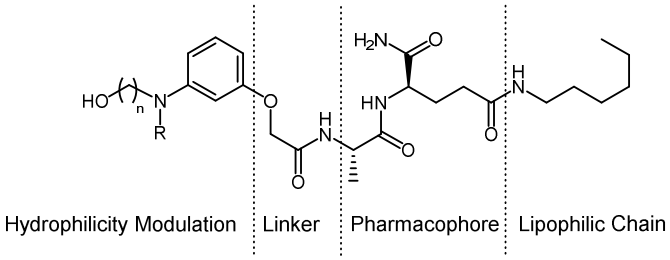

R	H	$(CH_2)_nOH$	CH_3CO	$CH_3(CH_2)_2CO$
n = 2	**1**	**2**	**3**	**4**
n = 3	**5**	**6**	**7**	**8**

Figure 3. Structural components of amphiphilic desmuramyl peptides (**1**–**8**).

Amphiphilic DMPs have not been explored yet. Herein, we report the synthesis of a group amphiphilic DMPs (**1** – **8**, Figure 3). The novel DMPs were examined for their effects on ICAM-1 (CD54) expression in THP-1 cells and the release of proinflammatory cytokine TNF-α. These amphiphilic DMPs demonstrated higher activity in the induction of TNF-α in THP-1 macrophages–than Murabutide which is a well-known NOD2 agonist. Furthermore, molecular docking studies indicate that all these DMPs bind NOD2 receptor well with similar docking scores (binding energy).

2. Results and Discussion

2.1. Syntheses

Amphiphilic DMPs were prepared by employing an efficient convergent synthetic approach. The synthesis began with 3-nitrophenol alkylation (Scheme 1). Briefly, *tert*-butyl 2-(3-aminophenoxy)acetate **9** was obtained by refluxing a mixture of *tert*-butyl 2-bromoacetate and 3-nitrophenol in acetone followed by catalytic hydrogenation of the nitro group via molecular hydrogen (H_2) and 10% palladium on charcoal.[57] Then, mono-*N*-alkylation of **9** was achieved

by refluxing it with 2-bromoethanol or 3-bromo-1-propanol in the presence of *N*,*N*-diisopropylethylamine (DIPEA) to afford mono-alkylated products **10** or **11** in good yield. Some di-*N*-alkylated products were also formed in this process, with their yields being less than 10%. Compound **10** was treated with sodium hydroxide (0.5 N) to give the free acid **20**. Alternatively, di-*N*-alkylated product **21** was obtained in high yield by refluxing **10** with an excess amount of 2-bromoethanol in the presence of DIPEA in acetonitrile, which was then hydrolysed to give free-acid **22**. Hydrophilicity modulation was achieved by reacting **10** and **11** with acetic anhydride, which afforded the less hydrophilic compounds **12** and **13**, respectively. The *tert*-butyl ester hydrolysis gave free acids **16** and **17**. NMR spectra of these compounds reveal duplication of signals, indicating the presence of a mixture of stereoisomers or conformers in the solution. Similarly, butyric acid reaction with **10** and **11** afforded **14** and **15**, which upon hydrolysis gave the free acids **18** and **19**.

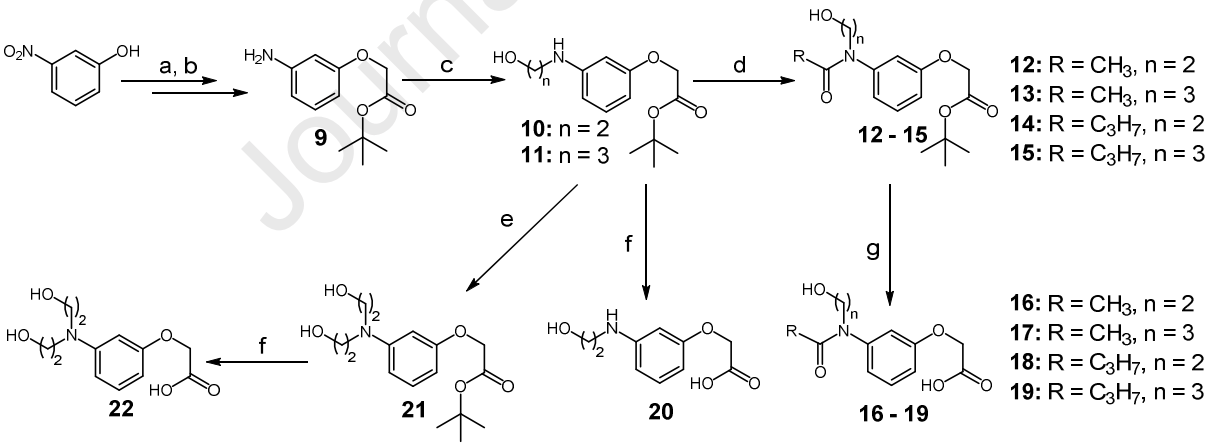

Scheme 1. a) *tert*-butyl 2-bromoacetate, K_2CO_3, $(CH_3)_2CO$, reflux, 81%; b) Palladium on charcoal, H_2, 94%; c) $Br(CH_2)_2OH$ or $Br(CH_2)_3OH$, *i*Pr_2NEt, C_2H_5OH, reflux, 58% for n = 2, 41% for n = 3; d) $(CH_3CO)_2O$ or $(C_3H_7CO)_2O$, CH_3OH, >99%; e) $Br(CH_2)_2OH$, *i*Pr_2NEt, CH_3CN, reflux, 71%; f-g) 0.5N NaOH, dioxane, 66% for **16**, 65% for **17**, >99% for **18-22**.

In the second phase of the convergent synthesis strategy, preparation of lipophilic dipeptide moiety was achieved. Previously, we demonstrated the preparation of (*R*)-4-((*S*)-2-aminopropanamido)-N^1-hexylpentanediamide **23** in five steps [57]. The free amine **23** was then coupled with **20** using TBTU in conjugation with *N*-methylmorpholine in DMF to give mono-alkylated DMP **1** in 38 % yield (Scheme 2). Similarly, di-alkylated DMP **2** was prepared by reacting **23** with acid **22** in 28 % yield. The cause of the poor yields was due to reactive hydroxyl groups present in the building blocks **20** and **22**. Owing to the poor yield encountered, an alternative strategy was adopted (Scheme 2). An equimolar mixture of free acid **20** or **22**, *N*-hydroxysuccinimide (NHS) and the free amine **23** were stirred in DMF-THF mixture at 0 °C. Then, dicyclohexylcarbodiimide (DCC) was added. NHS ester containing intermediate of the acid (**20**/**22**) was presumably generated by this new coupling method, which reacted more favorably with the amine group than the hydroxyl groups, resulting in higher yields for **1**–**2** (58 % and 51 %).

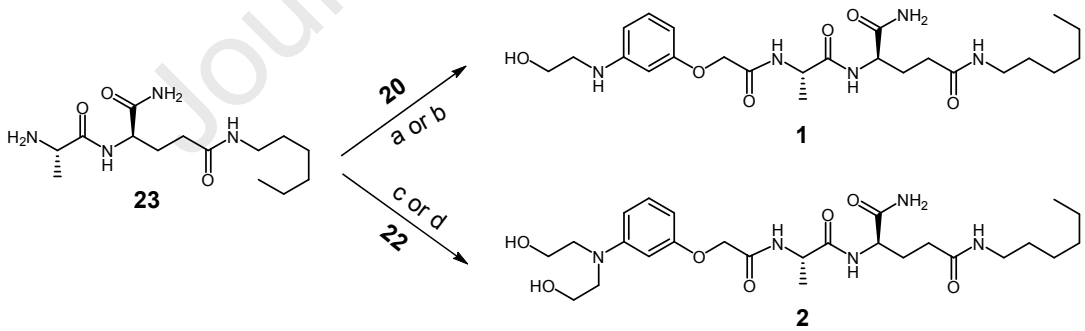

Scheme 2. a) TBTU, *N*-methylmorpholine, DMF, 38%; b) NHS, THF/DMF (3:2), DCC, 0 °C to rt, 58%; c) TBTU, *N*-methylmorpholine, DMF, 28%; d) NHS, THF/DMF (3:2), DCC, 0 °C to rt, 51%.

Similarly, an equimolar mixture of the free acid **16–19**, *N*-hydroxysuccinimide (NHS), the free amine **23**, and dicyclohexylcarbodiimide (DCC) were stirred in DMF-THF mixture at 0 °C to afford **3** and **4** and **7** and **8** in decent yield (Scheme 3).

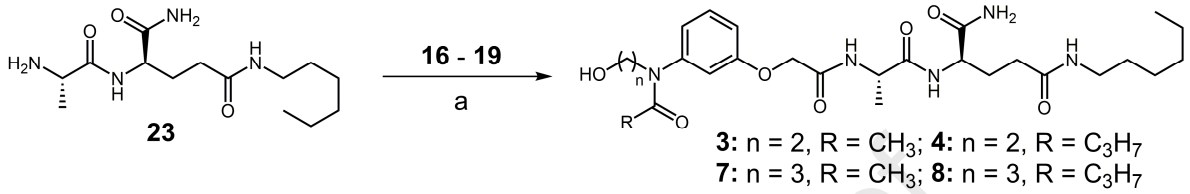

Scheme 3. a) NHS, THF/DMF (3:2), DCC, 0 °C to rt, 45% for **3**, 49% for **4**, 51% for **7**, and 48% for **8**.

Previously, we reported the synthesis of **5** and **6** using the same method (NHS/DCC coupling) to give 53% and 48% yield, respectively [57]. The *N*-acylated target molecules (**3**, **4**, **7**, and **8**) can also be readily prepared from compounds **1** and **5**. Thus, treatment of **1**/**5** with acetic anhydride or butyric anhydride afforded DMP **3**–**4** and **7**–**8** in quantitative yields (Scheme 4).

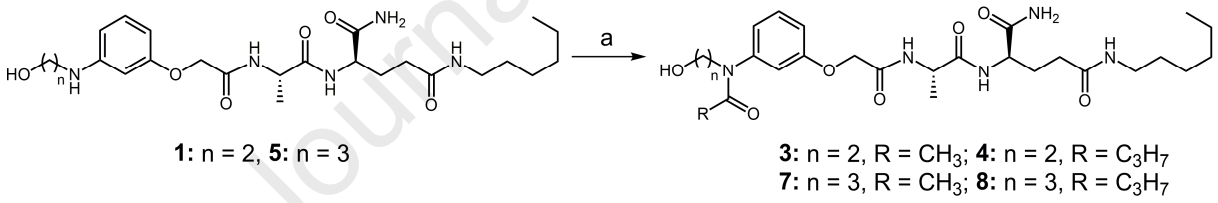

Scheme 4. a) $(CH_3CO)_2O$ or $(C_3H_7CO)_2O$, CH_3OH, rt, >99%.

^{1}H NMR studies of all compounds **1**–**8** display geminal proton-proton couplings ($^2J_{H\text{-}H}$) due to methylenoxy (OCH_2) protons of glycolic linker. This type of coupling usually appears as doublet pair if there are chiral centers in the molecule. Geminal coupling constant strongly depends on H–C–H bonds angle [58], and its value ranges from 0 Hz (for 125° angle) to 32 Hz (for 100° angle). For DMPs **1**–**8**, protons of the linker (OCH_2) are diastereotopic in nature which emerge as doublet pair at around 4.45 ppm, with ^2J value being 15 Hz in all cases (**Figure 4s–10s**).

Moreover, primary amide protons (NH_2 of the D-iso-Gln residue) in compounds **1–8** are not identical, since both protons appear as two singlets at δ 7.07 ppm and at δ 7.31 ppm due to prohibited amide bond rotation, thereby confirming the existence of intramolecular hydrogen bonding between glycolic carbonyl and α-carboxamide proton of D-iso-Gln [59].

2.2. Biological Studies

Innate immune cells contain specialized sensors, such as PRRs, to detect microbial pathogens [3]. These sensors are expressed either on cell surface in the form of Toll-like receptors (TLRs) or in the endosome e.g. NOD-like receptors (NLRs), which identify the harmful bacteria and viruses via PAMPs [60]. Upon recognition, PRRs prompt a signaling cascade setting off innate immune responses, including an increase in surface expression of the adhesion molecule ICAM-1 and pro-inflammatory cytokine release [4]. Although synergism of many NOD2 agonists, such as MDP or MDP-C with LPS, has been extensively reported in recent years, a crosstalk between DMPs and LPS in the regulation of ICAM-1 has hardly been explored [57,61,62]. Therefore, amphiphilic desmuramyl peptides were examined in combination with LPS for the induction of ICAM-1 in monocytic THP-1 cells. In the wake of preliminary results from DMP **5** and **6** [57], immunostimulatory prospects of the remaining compounds were further evaluated in THP-1 macrophages. The results were then compared with the effect of a well-known NOD2 agonist – murabutide.

In the first round of experiments, 20 μM concentration of murabutide or each compound was employed to stimulate monocytic THP-1 cells for 21 hours. However, ICAM-1 expression levels were significantly low (Supporting information, Figure 1s). Previously, MDP synergism with LPS has been reported [62]. In our experiments, amplification of lipopolysaccharide-

induced ICAM-1 in THP-1 monocytes was also observed by amphiphilic desmuramyl peptides **1**–**8** (Figure 2s–3s and Table 2s). Previously, 64% upregulation of ICAM-1 was observed at 16 μM concentration of compound **6** with LPS [57]. From the preliminary data, it was evident that compound **6** could enhance the lipopolysaccharide-induced ICAM-1 expression more effectively than other DMPs (Figure 3s). Further experiments were done with the macrophages, since monocytic THP-1 cells are weakly responsive to the immunostimulatory signals. 20 ng/ml of PMA (Phorbol 12-myristate-13-acetate) was used to ensure the sufficient differentiation of THP-1 monocytes into macrophages. When 20 μM of each amphiphilic DMPs **1**–**8** was incubated with differentiated THP-1 macrophages, the analysis of ICAM-1 expression indicated the highest mean fluorescence intensity of 905.38 under the effect of **8**, compared to a value of 602.95 for untreated cells (Figure 5). Cells treated with murabutide demonstrated the average value of 1436.05, which means that compounds **1**–**8** induced lower level of ICAM-1 expression than murabutide.

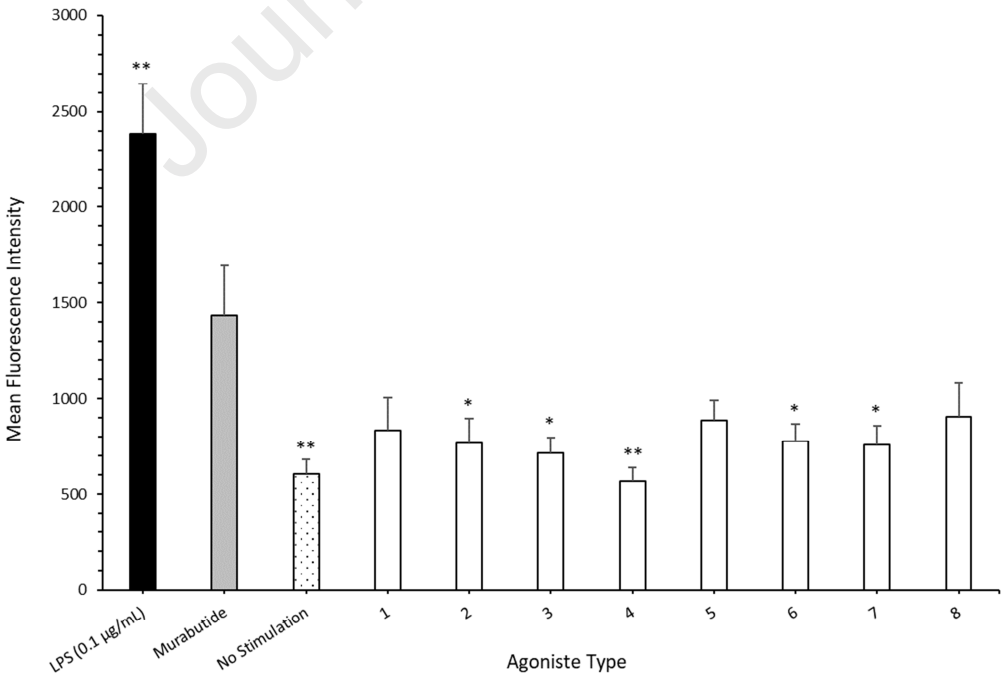

Figure 4. Cell surface expression of ICAM-1 in THP-1 macrophages treated with 20 µM of murabutide, or amphiphilic desmuramyl peptides **1**–**8**. FACS analysis (Flow cytometry) was employed for ICAM-1 measurements. The results of 3 separate experiments are shown as mean fluorescence intensity ± standard error mean (SEM). The one-way ANOVA was used for statistical analysis, whereas (∗) $p < 0.05$, and (∗∗) $p < 0.01$ in comparison with murabutide treated cells.

Previously, we demonstrated the strong effect of **6** on LPS-stimulated macrophages with higher ICAM-1 expression level than one induced by the well-known NOD2 agonist, murabutide [57]. In those experiments, 20 ng/mL of PMA was used to differentiate the monocytes, and the resulting macrophages were treated with different concentrations of **6** prior to LPS stimulation. Then, the stimulation with 8 µM concentration of **6** raised the overall expression of intracellular adhesion molecule 1 by 33 % as compared to LPS-only treated cells. This value was higher than that observed for **6** alone. Interestingly, similar ICAM-1 upregulation was also found in the case of murabutide, but it was less evident than that observed for **6** at 8 µM [57]. When lower concentrations (≤ 4 µM) of **6** were used to pre-treat the macrophages, no significant change in ICAM-1 expression level was observed. However, at higher concentrations (≥ 16 µM) of **6**, the down regulation of ICAM-1 occurred. The expression of ICAM-1 is mediated by the NF-κB transcriptional factor, and various inflammatory mediators such as TNF-α, γ-IFN and bacterial LPS [63]. Hence, the observed ICAM-1 upregulation can be attributed to the lipophilic chain in **6**, which enables its intracellular presence to potentiate LPS action via nuclear transcription factor mediated cytokines. It was therefore essential to quantify the pro-inflammatory cytokines released by the compounds **1**–**8** potentially mediated by the cytosolic NOD2 receptor.

When an agonistic ligand binds to its receptor, pro-inflammatory cytokines, nitric oxide and immunomodulating mediators are released [64]. Anti-infectious activity is generally mediated by a pro-inflammatory cytokine *viz.* tumour necrosis factor (TNF-α). *In vitro* studies suggest that

numerous muropeptides induce TNF-α production in myeloid-derived cells and human monocytes. For example, Boons *et al.* reported TNF-α gene expression in human monocytic cell lines by employing muramyl tripeptides [65]. Similarly, desmuramyl peptides and tuftsin/retro-tuftsin containing nor-MDP derivatives were able to stimulate the secretion of TNF-α in PBMCs and lymphocytes [66]. Therefore, we decided to measure TNF-α production in THP-1 macrophages to assess the immunostimulatory potential of amphiphilic DMPs (**1–8**). These compounds were able to induce significant levels of TNF-α. Maximum response level was observed at 15 μM concentration (Figure 6). This response decreased by further increase in the concentration of the agonist. For example, 2-hydroxyethyl containing amphiphilic DMPs **1–4** used at a concentration of 15 μM induced TNF-α release of 3226 ± 297 pg/mL, 3111 ± 24 pg/mL, 3342 ± 91 pg/mL and 2806 ± 146 pg/mL, respectively. These values are considerably higher than those induced by 15 μM murabutide (2694 ± 271 pg/mL). Similarly, at 15 μM concentration, 3-hydroxypropyl containing amphiphilic DMPs **5–8** demonstrate average TNF-α release values of 3622 ± 371 pg/mL, 3306 ± 231 pg/mL, 2902 ± 335 pg/mL and 3105 ± 400 pg/mL respectively, which were higher than those observed for all 2-hydroxyethyl containing DMPs except **3**. Interestingly, higher concentrations of amphiphilic DMPs (e.g. 30 μM) dampened the release of TNF-α (Figure 6). In the previous experiments, low values of LPS-induced ICAM-1 expression were observed at higher concentrations of amphiphilic DMP **6**, although no indication of cell deaths was found [57]. Higher doses of MDP have also been reported to show a similar effect [67]. Further *in vivo* studies are required to comprehend the mechanistic details of the immunomodulatory activity by amphiphilic DMPs and their therapeutic potential.

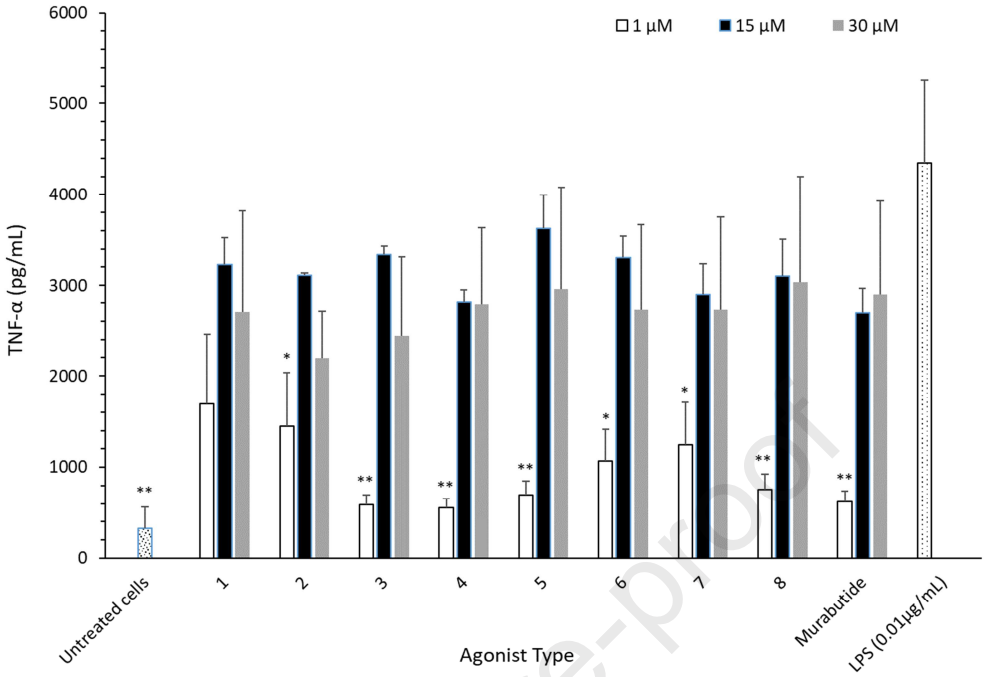

Figure 5. TNF-α release in macrophages stimulated by DMPs (**1–8**). PMA concentration of 20ng/mL was used to differentiate monocytes into macrophages. Then for the next 24 hours, stimulation was done with 1, 15, 30 µM of each DMP. Enzyme-linked immunosorbent assay (ELISA) was used to estimate TNF-α in the supernatant. Two separate experiments were used to express the results ± SEM. One-way ANOVA was used to find the statistically significant differences, whereas (∗) $p < 0.05$, (∗∗) $p < 0.01$ vs 15 µM murabutide treated cells.

2.3. Computational Studies

To get deeper insights into the structural requirements of amphiphilic desmuramylpeptides (DMPs), molecular docking study was performed using Nucleotide-Binding Oligomerization Domain-Containing Protein 2 receptor (NOD2). The crystal structure of human NOD2 has not been reported yet. Therefore, homology modelling was carried out by using a web-server, SWISS-MODEL [68]. For the identification of template structure, an NCBI protein-Blast search [69] was performed against uniport reference sequence: Q9HC29. The BLAST search identified rabbit (*Oryctolague cuniculus*) NOD2 protein (PDB ID: 5IRN) [70] as

the best match for human NOD2 which shares 86% identity with the target protein (Figure 9s). The quality of the model was assessed to confirm if it was suitable for performing further studies. For this purpose, online quality evaluation tools, such as ERRAT, PROCHECK and Verify-3D [71] were used (Figure 4s). The plot showed the overall refinement of the modelled structures as most of the residues were present in the core region while only one outlier Gln968 is found which is far from the active site. Superimposition of homology model with the template is illustrated in Figure 7A. The calculated root means square deviation (RMSD) of NOD2 model against 5IRN is 0.676 Å.

Table 2. Binding energy score of DMPs (**1**–**8**) and their interactions with the residues of NOD2 receptor

DMP	Dock Score (Kcal/mol)	Hydrogen bonding	Hydrophobic/π interactions
1	-7.95	Gly879 with α-carboxamide of D-iso-Gln Gly905 with α-carboxamide of D-iso-Gln	Aryl group of Trp931 with *N*-hexyl chain Aryl group of Trp907 with $(CH_2)_2$ of D-iso-Gln Cation-π interaction between Arg823 and N-aryl ring
2	-7.92	Arg823 with aryl amine Arg877 with α-carboxamide of D-iso-Gln	Aryl group of Phe903 with *N*-hexyl chain Aryl group of Trp907 with methyl of L-Ala
3	-7.52	Arg823 with α-carboxamide of D-iso-Gln Ser991 with acetyl group	Aryl group of Arg877 with *N*-hexyl chain Aryl group of Phe851 with $(CH_2)_2$ of D-iso-Gln Aryl group of Trp907 with $(CH_2)_2$ of D-iso-Gln
4	-7.94	Arg823 with amide of glycolic linker Asn880 with butyryl group	Aryl group of Tyr799 with *N*-hexyl chain Aryl group of Phe851 with methyl of L-Ala Alkyl chain of Lys271 with *N*-aryl ring
5	-7.42	Gly879 with α-carboxamide of D-iso-Gln Gly905 with α-carboxamide of D-iso-Gln Glu959 with aryl amine	Alkyl chain of Lys271 with *N*-hexyl chain Aryl group of Trp931 with methyl of L-Ala
6	-7.83	Arg877 with *N*-hexyl chain Asn880 with hydroxy ethyl group	Aryl group of Trp931 with *N*-hexyl chain Aryl group of Trp907 with methyl of L-Ala
7	-7.77	Glu959 with amide of glycolic linker Trp931 with the amide of L-Ala	Aryl group of Phe851 with *N*-hexyl chain Aryl group of Trp907 with $(CH_2)_2$ of D-iso-Gln Alkyl chain of Lys986 with methyl of acetyl group
8	-7.96	Arg877 with the amide of L-Ala Trp907 with butyryl group Lys989 with hydroxy propyl group	Aryl group of Trp931 with *N*-hexyl chain π - π Interaction between Phe851 and *N*-aryl ring

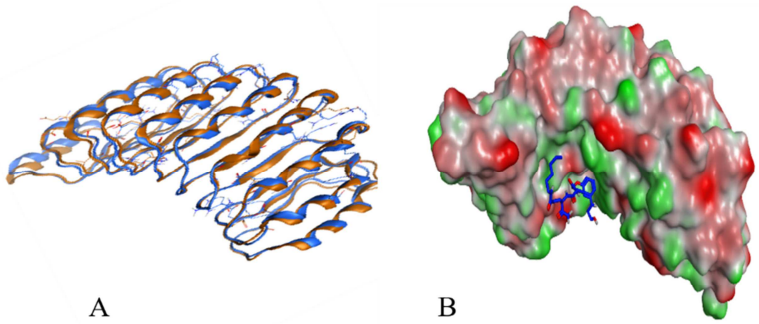

Figure 6. (A) Superimposition of crystal structure (brown) and modeled structure (blue); (B) Surface representation of the NOD2-LRR domain with compound **1** (in blue) showing the concave binding pocket.

The docking results indicate that all DMPs (**1**–**8**) bind well to NOD2 receptor, with their dock scores (binding energy) ranging from -7.96 to -7.42 kcal/mol. Although these compounds show similar dock scores, they display different binding modes through a number of hydrophilic and hydrophobic interactions with the crucial residues in the binding site of the receptor (Table 2, Figure 8). The majority of hydrogen bond interactions were observed between L-Ala-D-iso-Gln residue of DMPs and the surrounding amino acids of NOD2 binding pocket, which means that this dipeptide moiety is essential for the activity of **1**–**8**. The α-carboxamide group of D-iso-Gln in compound **1**, **2**, **3** and **5** was implicated in H-bonding with the residues Gly823, Gly879 and Gly905. In contrast, L-alanine in compound **7** and **8** formed H-bonding with Arg877 and Trp931 residues. The -CH_2CH_2- moiety of D-iso-Gln in the dipeptide was also involved in hydrophobic/π interactions with Phe851 and Trp907 in compound **1**, **3** and **7**, while the methyl group of L-Ala in **2** and **4**–**6** interacted with Phe851, Trp907 and Trp931. Hydrophilic arene in compound **2** and **5** was found interacting with Arg823 and Glu959 via H-bonding. The aryl amine in **1** established the cation-π interaction with Arg823 in NOD2 binding pocket. Furthermore, hydrophobic interactions involving the lipophilic *N*-hexyl chain were observed in all DMP molecules (**1**–**8**). The hexyl chain in compound **5** interacted with the lipophilic alkyl chain of Lys271 while in all other compounds

the hexyl chain was interacting with an aromatic ring of several Phe, Trp, and Arg residues. Interestingly, besides the cation-π interaction mentioned above for compound **1**, hydrophobic/π interactions involving the aryl ring of the DMPs were only found in compounds **4** and **8**, both of which bearing a butyryl group on the nitrogen atom of the aryl amine.

Taken together, the results of docking studies suggest that all DMPs (**1** – **8**) bind into the concave hydrophobic cavity of NOD2-LRR domain and interact with the crucial residues of the NOD2. In the cavity, they adopt different conformations due to their hydroxyalkyl and the lipophilic chains, which consequently leads to their different modes of interaction with the receptor. Overall, docking results provide structural insight into the binding mode of newly synthesized DMPs, which highlights the importance of the dipeptide moiety (L-Ala-D-iso-Gln) in conjugation with other structural elements including the alkyl amide chain, the aryl amine group, the hydroxylalkyl group, and the N-acyl group. These findings will be useful for designing new DMPs with higher binding affinity to the NOD2 receptor, ultimately leading towards improved biological activities.

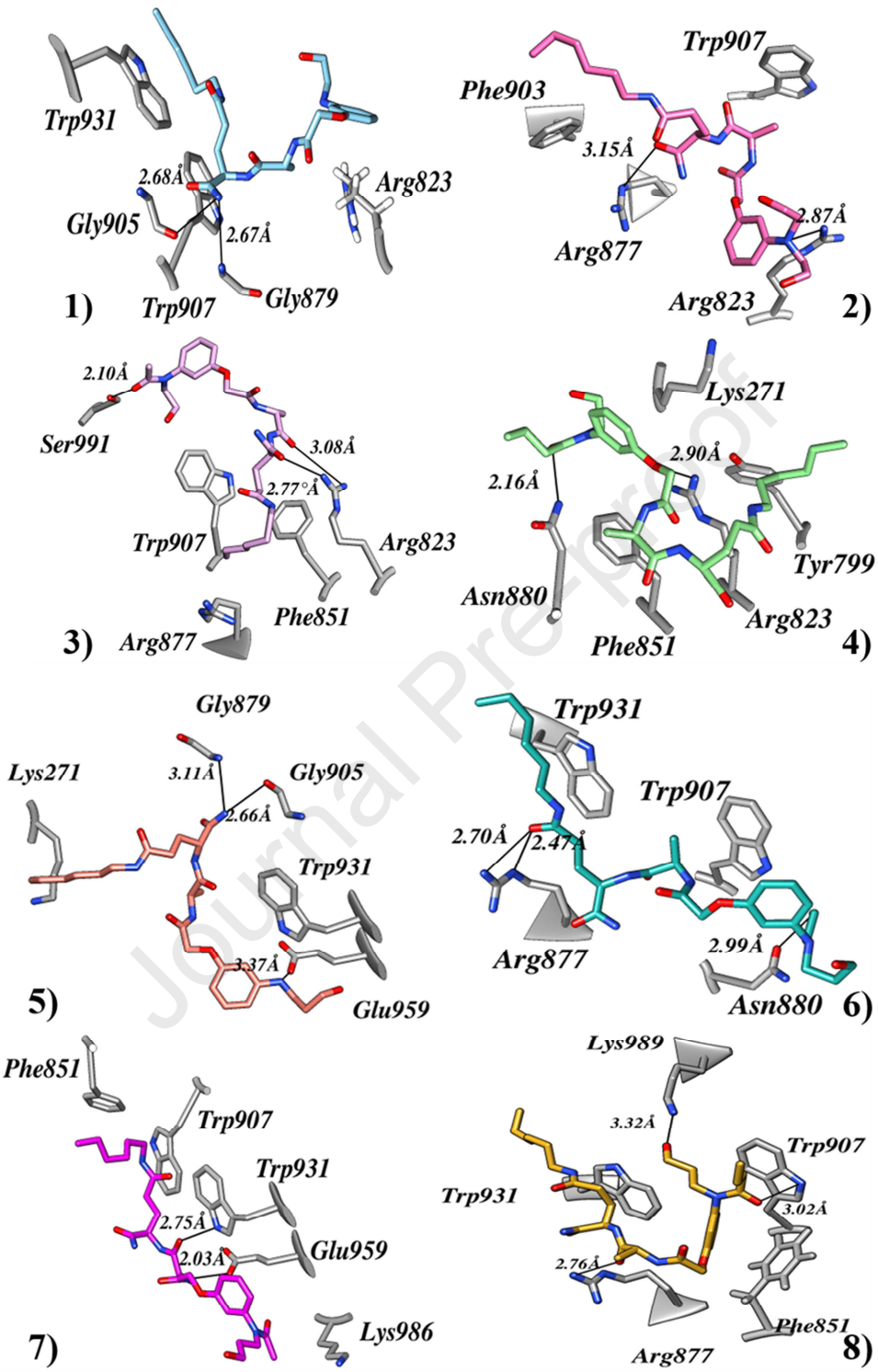

Figure 7. Molecular docking of DMPs (**1–8**). The stick model of different colors shows the compounds, and the key amino acid residues of NOD2 receptor around compounds have been displayed in grey stick model.

3. Conclusion

In summary, new class of desmuramyl peptides containing hydrophilic arene moiety and lipophilic chain were prepared. These compounds were primarily assessed *in vitro* by investigating their synergistic effect on LPS-induced expression of surface glycoprotein *viz.* ICAM-1 (CD54). In addition, pro-inflammatory cytokine (TNF-α) release in THP-1 macrophages was measured. The novel compounds were found to upregulate the expression of LPS-induced ICAM-1 (CD54), and could trigger the release of higher TNF-α levels than murabutide. The overall similitude in the immunostimulatory activity of the amphiphilic DMPs and murabutide is remarkable, especially when there are huge structural differences among them. *In silico* studies also revealed that all the ligands interacted with crucial residues of NOD2-LRR binding domain. Additional work is needed to demonstrate whether these compounds reveal the immunomodulatory effect via NOD2 receptor activation. Their immunomodulating potential needs further assessment through the profiling of other cytokines in different immune cells. *In vivo* studies may be ensued to investigate the therapeutic potential of the amphiphilic DMPs as immunomodulatory/immunostimulatory agents.

4. Experimental Section

4.1. Reagents and instruments

Most of the chemicals, obtained from Sigma-Aldrich (Merck KGaA), were used without further purifications. Analytical grade solvents were employed, and the air-sensitive compounds were handled using the standard Schlenk techniques. Murabutide was obtained from Sigma-Aldrich, and LPS *E. coli* O111:B4 was purchased from InvivoGen, San Diego, CA. DMSO was used to dissolve the synthetic DMPs followed by their water reconstitution and storage at -20 °C.NMR

spectra were recorded with Bruker® Avance (400 MHz) and on a Varian® Unity Inova (500 MHz) spectrometer in deuterated solvents.

4.2. Syntheses procedures and structure characterization

For the cleavage of *tert*-Butoxycarbonyl group, ice-cooled dichloromethane solution of Boc containing compound was treated with trifluoroacetic acid (TFA). Stirring was continued until consumption of all the starting material which was confirmed via TLC monitoring. The solution was then concentrated *in vacuo* followed by its neutralization with an aqueous 10% $NaHCO_3$ solution. Subsequent solvent removal gave the crude product. Whenever the desired product was an amine salt, the TFA containing solvent was evaporated *in vacuo*. Then methanol co-evaporation was then used to eliminate the residual TFA and get the product quantitatively. Similarly, ester hydrolysis of **10 – 15** and **21** was done by dropwise addition of aqueous NaOH (0.5 N, 2 ml) to an ice-cooled solution of dioxane (3 mL) containing the above-mentioned compounds. Hydrolysis was monitored with TLC until consumption of all the starting material. The reaction mixture was subsequently neutralized with dilute HCl (0.5 N) and the solvent removed under reduced pressure. Absolute ethanol was employed to filter off the salt. Procedure for the synthesis of compounds **5**, **6**, **9**, **11**, **21**, **23**, **25** and **26** can be traced back from our previously published work [57].

*4.2.1. (R)-N^1-hexyl-4-((S)-2-(2-(3-((2-hydroxyethyl)amino)phenoxy)acetamido) propanamido)pentanediamide (**1**)*

A mixture of DMF (3 mL) and **23** (0.1 g, 0.33 mmol) was added to TBTU (0.12 g, 0.36 mmol), *N*-methylmorpholine (0.11 ml, 1.0 mmol) and **20** (0.07 g, 0.33 mmol) containing DMF solution (5 mL). After vigorous stirring (18 h, room temperature), the solvent was removed *in vacuo*. Air-

sensitive **1** (0.062 g, 38 %) was obtained as white powder after the residue purification over flash silica column (Chloroform/Methanol, 5:1). Alternatively, DMF (2 mL) solution of **20** (0.07 g, 0.33 mmol) was mixed to an ice-cooled THF (3 mL) containing 1-hydroxypyrrolidine-2,5-dione (0.04 g, 0.33 mmol) and **23** (0.1 g, 0.33 mmol). This was followed by the addition of dicyclohexylcarbodiimide (0.07 g, 0.33 mmol). Overnight stirring at room temperature resulted in dicyclohexyl urea precipitates. After filtration, the solvents were removed *in vacuo*. Residue thus obtained was purified over flash silica column (Chloroform/Methanol, 5:1), which afforded air-sensitive **1** (0.095 g, 58 %) as white powder: R_f = 0.42; ^{1}H NMR (500 MHz, $(CD_3)_2SO$): δ 0.84 (t, 3H, J = 7 Hz, $C\underline{H}_3CH_2$), 1.21 (m, 6H, $CH_3(C\underline{H}_2)_3$), 1.24 (d, 3H, J = 7 Hz, $CHC\underline{H}_3$), 1.34 (quint, 2H, J = 8 Hz, $CH_3(CH_2)_3C\underline{H}_2$), 1.68 (m, 1H, CHC<u>H</u>H), 1.92 (m, 1H, CHCH<u>H</u>), 2.05 (t, 2H, J = 7 Hz, $CHCH_2C\underline{H}_2$), 2.98 (m, 2H, $CONHC\underline{H}_2$), 3.04 (q, 2H, J = 6 Hz, $C\underline{H}_2OH$), 3.52 (q, 2H, J = 6 Hz, $NHC\underline{H}_2CH_2OH$), 4.10 (td, 1H, J = 5, 8 Hz, $C\underline{H}CH_2$), 4.35 (quint., 1H, J = 7 Hz, $C\underline{H}CH_3$), 4.40 (dd, 2H, J = 15 Hz, OCH_2), 4.68 (t, 1H, J = 5 Hz, OH), 5.54 (t, 1H, J = 5 Hz, $N\underline{H}CH_2CH_2CH_2OH$), 6.10 (d, 1H, J = 8 Hz, OCC<u>H</u>CHCH), 6.15 (s, 1H, CCHC), 6.20 (d, 1H, J = 2, 8 Hz, OCCHCHC<u>H</u>), 6.94 (t, 1H, J = 8 Hz, OCCHC<u>H</u>CH), 7.08 (s, 1H, NH_2), 7.31 (s, 1H, NH_2), 7.77 (t, 1H, J = 5 Hz, $CON\underline{H}CH_2$), 8.07 (d, 1H, J = 7 Hz, $CH_3CHN\underline{H}$), 8.22 (d, 1H, J = 8 Hz, CHN<u>H</u>CO). ^{13}C NMR (125 MHz, $(CD_3)_2SO$): δ 13.98 ($\underline{C}H_3CH_2$), 18.39 ($\underline{C}H_3CH$), 22.11 ($\underline{C}H_2CH_3$), 26.13 (CH_2), 27.70 (CH_2), 29.10 (CH_2), 31.05 (CH_2), 31.81 (CH_2), 38.53 (NCH_2), 45.55 ($NHCH_2$), 48.16 ($\underline{C}HCH_3$), 52.23 ($\underline{C}HCH_2$), 59.61 (CH_2OH), 66.66 (OCH_2), 98.36 (CHCH<u>C</u>H), 101.61 (<u>C</u>HCHCH), 106.05 (C<u>C</u>HC), 129.64 (CH<u>C</u>HCH), 150.35 (N<u>C</u>CH), 158.83 (NCCH<u>C</u>), 167.73 ($CH_3CH\underline{C}$=O), 171.33 ($CH_2\underline{C}$=O), 171.95 ($OCH_2\underline{C}$=O), 173.30 ($NH_2\underline{C}$=O); MALDI-TOF (*m/z*) Calcd for $C_{24}H_{39}N_5O_6$ $[M+Na]^+$: 516.2798, found: 516.2229.

*4.2.2. (R)-4-((S)-2-(2-(3-(bis(2-hydroxyethyl)amino)phenoxy)acetamido)propanamido)-N[1]-hexylpentanediamide (**2**)*

A mixture of DMF (3 mL) and **23** (0.1 g, 0.33 mmol) was added to TBTU (0.12 g, 0.36 mmol), *N*-methylmorpholine (0.11 ml, 1.0 mmol) and **22** (0.08 g, 0.33 mmol) containing DMF solution (5 mL). After vigorous stirring (18 h, RT), the solvent was removed *in vacuo*. Air-sensitive **2** (0.052 g, 28 %) was obtained as white powder after the residue purification over flash silica column (Chloroform/Methanol, 5:1). Alternatively, DMF (2 mL) solution of **22** (0.08 g, 0.33 mmol) was mixed to an ice-cooled THF (3 mL) containing 1-hydroxypyrrolidine-2,5-dione (0.04 g, 0.33 mmol) and **23** (0.1 g, 0.33 mmol). This was followed by the addition of dicyclohexylcarbodiimide (0.07 g, 0.33 mmol). Overnight stirring at room temperature resulted in dicyclohexyl urea precipitates. After filtration, the solvents were removed *in vacuo*. Residue thus obtained was purified over flash silica column (Chloroform/Methanol, 5:1), which afforded an air-sensitive compound **2** (0.091 g, 51 %) as white powder: R_f = 0.37; ^{1}H NMR (500 MHz, $(CD_3)_2SO$): δ 0.84 (t, 3H, J = 7 Hz, $C\underline{H}_3CH_2$), 1.22 (m, 6H, $CH_3(C\underline{H}_2)_3$), 1.24 (d, 3H, J = 7 Hz, $CHC\underline{H}_3$), 1.33 (quint, 2H, J = 8 Hz, $CH_3(CH_2)_3C\underline{H}_2$), 1.69 (m, 1H, $CHC\underline{H}H$), 1.93 (m, 1H, $CHCH\underline{H}$), 2.06 (t, 2H, J = 7 Hz, $CHCH_2C\underline{H}_2$), 2.98 (m, 2H, $NHC\underline{H}_2$), 3.37 (m, 4H, $C\underline{H}_2OH$), 3.50 (q, 4H, J = 6 Hz, $NC\underline{H}_2$), 4.10 (td, 1H, J = 5, 9 Hz, $C\underline{H}CH_2$), 4.35 (quint., 1H, J = 7 Hz, $C\underline{H}CH_3$), 4.43 (d, 2H, J = 15 Hz, OCH_2), 4.73 (t, 2H, J = 5 Hz, OH), 6.15 (d, 1H, J = 8 Hz, $OCC\underline{H}CHCH$), 6.23 (s, 1H, J = 2 Hz, CCHC), 6.29 (d, 1H, J = 8 Hz, $OCCHCHC\underline{H}$), 7.01 (t, 1H, J = 8 Hz, $OCCHC\underline{H}CH$), 7.06 (s, 1H, NH_2), 7.29 (s, 1H, NH_2), 7.75 (t, 1H, J = 5 Hz, $CON\underline{H}CH_2$), 8.09 (d, 1H, J = 7 Hz, $CHN\underline{H}$), 8.21 (d, 1H, J = 8 Hz, $CHN\underline{H}$). ^{13}C NMR (125 MHz, $(CD_3)_2SO$): δ 14.39 ($\underline{C}H_3CH_2$), 18.79 ($\underline{C}H_3CH$), 22.51 ($\underline{C}H_2CH_3$), 26.55 (CH_2), 28.13 (CH_2), 29.52 (CH_2), 31.46 (CH_2), 32.25 (CH_2), 38.97 (NCH_2), 48.64 ($\underline{C}HCH_3$), 52.68 ($\underline{C}HCH_2$),

53.78 ($NHCH_2$), 58.60 (CH_2OH), 67.23 (OCH_2), 98.77 (CHCH<u>C</u>H), 101.52 (<u>C</u>HCHCH), 105.54 (C<u>C</u>HC), 130.22 (CH<u>C</u>HCH), 149.76 (N<u>C</u>CH), 159.42 (NCCH<u>C</u>), 168.17 (CH_3CH<u>C</u>=O), 171.76 (CH_2<u>C</u>=O), 172.38 (OCH_2<u>C</u>=O), 173.70 (NH_2<u>C</u>=O); MALDI-TOF (*m/z*) Calcd for $C_{26}H_{43}N_5O_7$ $[M+Na]^+$: 560.3060, found: 560.2590.

*4.2.3. (R)-N[1]-hexyl-4-((S)-2-(2-(3-(N-(2-hydroxyethyl)acetamido)phenoxy)acetamido) propanamido)pentanediamide (**3**)*

DMF (2 mL) solution of **16** (0.08 g, 0.33 mmol) was mixed to an ice-cooled THF (3 mL) containing 1-hydroxypyrrolidine-2,5-dione (0.04 g, 0.33 mmol) and **23** (0.1 g, 0.33 mmol). This was followed by the addition of dicyclohexylcarbodiimide (0.07 g, 0.33 mmol). Overnight stirring at room temperature resulted in dicyclohexyl urea precipitates. After filtration, the solvents were removed *in vacuo*. Residue thus obtained was purified over flash silica column (Chloroform/Methanol, 5:1), which afforded an air-sensitive compound **3** (0.08 g, 45 %) as white powder. Alternatively, methanol (5 mL) containing **1** (0.05 g, 0.1 mmol) was stirred with acetic anhydride (0.01 ml, 0.1 mmol) at room temperature, which afforded **3** in quantitative yield: R_f = 0.40; ^{1}H NMR (500 MHz, $(CD_3)_2SO$): δ 0.81 (t, 3H, J = 7 Hz, C<u>H</u>$_3$CH$_2$), 1.19 (m, 6H, CH_3(C<u>H</u>$_2$)$_3$), 1.23 (d, 3H, J = 7 Hz, CHC<u>H</u>$_3$), 1.32 (m, 2H, $CH_3(CH_2)_3$C<u>H</u>$_2$), 1.66-1.70 (m, 4H, CHC<u>H</u>H, CH_3CO), 1.90 (m, 1H, CHCH<u>H</u>), 2.05 (t, 2H, J = 7 Hz, $CHCH_2$C<u>H</u>$_2$), 2.96 (m, 2H, CONHC<u>H</u>$_2$), 3.41 (m, 4H, C<u>H</u>$_2$OH, NHC<u>H</u>$_2$CH$_2$OH), 4.07 (td, 1H, J = 5, 8 Hz, C<u>H</u>CH$_2$), 4.31 (quint., 1H, J = 7 Hz, C<u>H</u>CH$_3$), 4.54 (dd, 2H, J = 15 Hz, OCH_2), 4.78 (s, 1H, OH), 6.89-6.99 (m, 3H, CH_{Ar}), 7.07 (s, 1H, NH_2), 7.33 (s, 1H, NH_2), 7.36 (m, 1H, CH_{Ar}), 7.82 (t, 1H, J = 5 Hz, N<u>H</u>CH$_2$), 8.25 (t, 2H, J = 8 Hz, CHN<u>H</u>). ^{13}C NMR (125 MHz, $(CD_3)_2SO$): δ 14.31 (<u>C</u>H$_3$CH$_2$), 18.54 (<u>C</u>H$_3$CH), 22.43 (<u>C</u>H$_2$CH$_3$), 22.87 (CH_2), 26.45 (CH_2), 27.98 (CH_2), 29.37 (<u>C</u>H$_3$CO),

31.37 (CH_2), 32.18 (CH_2), 38.97 (NCH_2), 48.74 ($\underline{C}HCH_3$), 51.15 ($\underline{C}HCH_2$), 52.67 (CH_2OH), 58.34 (NCH_2), 67.18 (OCH_2), 114.38 (CHCH$\underline{C}$H), 115.03 ($\underline{C}$HCHCH), 121.32 (C$\underline{C}$HC), 130.70 (CH$\underline{C}$HCH), 144.72 (N$\underline{C}$CH), 158.68 (NCCH$\underline{C}$), 167.89 ($CH_3CH\underline{C}$=O), 170.04 ($CH_2\underline{C}$=O), 172.02 ($OCH_2\underline{C}$=O), 172.46 ($CH_3\underline{C}$=O), 173.88 ($NH_2\underline{C}$=O); MALDI-TOF (*m/z*) Calcd for $C_{26}H_{41}N_5O_7$ $[M+Na]^+$: 558.2904, found: 558.2421.

*4.2.4. (R)-N[1]-hexyl-4-((S)-2-(2-(3-(N-(2-hydroxyethyl)butyramido)phenoxy)acetamido) propanamido) pentanediamide (**4**)*

DMF (2 mL) solution of **18** (0.09 g, 0.33 mmol) was mixed to an ice-cooled THF (3 mL) containing 1-hydroxypyrrolidine-2,5-dione, (0.04 g, 0.33 mmol) and **23** (0.1 g, 0.33 mmol). This was followed by the addition of dicyclohexylcarbodiimide (0.07 g, 0.33 mmol). Overnight stirring at room temperature resulted in dicyclohexyl urea precipitates. After filtration, the solvents were removed *in vacuo*. Residue thus obtained was purified over flash silica column (Chloroform/Methanol, 5:1), which afforded an air-sensitive compound **4** (0.092 g, 49 %) as white powder. Alternatively, methanol (5 mL) containing **1** (0.05 g, 0.1 mmol) was stirred with butyric anhydride (0.017 ml, 0.1 mmol) at room temperature, which afforded **4** in quantitative yield: R_f = 0.38; ^{1}H NMR (500 MHz, $(CD_3)_2SO$): δ 0.76 (t, 3H, J = 6 Hz, $C\underline{H_3}(CH_2)_2CO$), 0.84 (t, 3H, J = 7 Hz, $C\underline{H_3}CH_2$), 1.24 (m, 8H, $CH_3(C\underline{H_2})_4$), 1.26 (d, 3H, J = 7 Hz, $CHC\underline{H_3}$), 1.35 (m, 2H, $CH_3(CH_2)_3C\underline{H_2}$), 1.45 (m, 2H, $CH_3C\underline{H_2}CH_2CO$), 1.72 (m, 1H, CHC$\underline{H}$H), 1.96 (m, 1H, CHCH$\underline{H}$), 2.07 (t, 2H, J = 7 Hz, $CHCH_2C\underline{H_2}$), 3.00 (m, 2H, $CONHC\underline{H_2}$), 3.44 (q, 2H, J = 6 Hz, $C\underline{H_2}OH$), 3.65 (t, 2H, J = 6 Hz, $NHC\underline{H_2}CH_2OH$), 4.13 (td, 1H, J = 5, 8 Hz, $C\underline{H}CH_2$), 4.37 (quint., 1H, J = 7 Hz, $C\underline{H}CH_3$), 4.57 (dd, 2H, J = 15 Hz, OCH_2), 4.74 (s, 1H, OH), 6.89-6.97 (m, 3H, CH_{Ar}), 7.07 (s, 1H, NH_2), 7.33 (s, 1H, NH_2), 7.35 (t, 1H, J = 3 Hz, CH_{Ar}), 7.82 (t, 1H, J = 5

Hz, N<u>H</u>CH$_2$), 8.26 (t, 2H, J = 8 Hz, CHN<u>H</u>). ^{13}C NMR (125 MHz, (CD$_3$)$_2$SO): δ 13.78 (<u>C</u>H$_3$(CH$_2$)$_2$CO), 14.07 (<u>C</u>H$_3$(CH$_2$)$_5$NH), 18.37 (<u>C</u>H$_3$CH), 22.19 (<u>C</u>H$_2$CH$_3$), 26.21 (CH$_2$), 27.76 (CH$_2$), 29.15 (CH$_2$), 31.12 (CH$_2$), 31.88 (CH$_2$), 35.67 (CH$_2$), 38.65 (NCH$_2$), 48.38 (<u>C</u>HCH$_3$), 50.97 (<u>C</u>HCH$_2$), 52.34 (CH$_2$), 58.08 (CH$_2$OH), 66.89 (OCH$_2$), 107.23 (NHCH$_2$), 114.07 (CHCH<u>C</u>H), 114.98 (<u>C</u>HCHCH), 121.30 (C<u>C</u>HC), 130.39 (CH<u>C</u>HCH), 144.08 (N<u>C</u>CH), 158.44 (NCCH<u>C</u>), 167.47 (CH$_3$CH<u>C</u>=O), 169.52 (CH$_3$(CH$_2$)$_2$<u>C</u>=O), 171.57 (CH$_2$<u>C</u>=O), 172.08 (OCH$_2$<u>C</u>=O), 173.47 (NH$_2$<u>C</u>=O); MALDI-TOF (*m/z*) Calcd for $C_{28}H_{45}N_5O_7$ $[M+Na]^+$: 586.3217, found: 586.2845.

*4.2.5. (R)-N^1-hexyl-4-((S)-2-(2-(3-(N-(3-hydroxypropyl)acetamido)phenoxy)acetamido) propanamido) pentanediamide (**7**)*

DMF (2 mL) solution of **17** (0.09 g, 0.33 mmol) was mixed to an ice-cooled THF (3 mL) containing 1-hydroxypyrrolidine-2,5-dione (0.04 g, 0.33 mmol) and **23** (0.1 g, 0.33 mmol). This was followed by the addition of dicyclohexylcarbodiimide (0.07 g, 0.33 mmol). Overnight stirring at room temperature resulted in dicyclohexyl urea precipitates. After filtration, the solvents were removed *in vacuo*. Residue thus obtained was purified over flash silica column (Chloroform/Methanol, 10:1), which gave an air-sensitive compound **7** (0.093 g, 51 %) as white powder. Alternatively, methanol (5 mL) containing **7** (0.05 g, 0.1 mmol) was stirred with acetic anhydride (0.01 ml, 0.1 mmol) at room temperature, which afforded **7** in quantitative yield: R_f = 0.20; ^{1}H NMR (500 MHz, (CD$_3$)$_2$SO): δ 0.86 (t, 3H, J = 7 Hz, C<u>H</u>$_3$CH$_2$), 1.24 (m, 6H, CH$_3$(C<u>H</u>$_2$)$_3$), 1.26 (d, 3H, J = 7 Hz, CHC<u>H</u>$_3$), 1.35 (quint., 2H, J = 7 Hz, CH$_3$(CH$_2$)$_3$C<u>H</u>$_2$), 1.53 (quint, 2H, J = 7 Hz, C<u>H</u>$_2$CH$_2$OH), 1.67-1.72 (m, 4H, CHC<u>H</u>H, CH$_3$CO), 1.90 (td, 1H, J = 7, 13 Hz, CHCH<u>H</u>), 2.05 (t, 2H, J = 7 Hz, CHCH$_2$C<u>H</u>$_2$), 2.96 (m, 2H, CONHC<u>H</u>$_2$), 3.63 (t, 2H, J = 7

Hz, C$\underline{H}_2$OH), 4.10 (td, 1H, J = 5, 8 Hz, C$\underline{H}$CH$_2$), 4.35 (quint., 1H, J = 7 Hz, C$\underline{H}$CH$_3$), 4.39 (s, 1H, OH), 4.54 (dd, 2H, J = 15 Hz, OCH$_2$), 6.87-6.94 (m, 3H, CH$_{Ar}$), 7.07 (s, 1H, NH$_2$), 7.28 (s, 1H, NH$_2$), 7.35 (t, 1H, J = 8 Hz, CH$_{Ar}$), 7.77 (t, 1H, J = 5 Hz, N$\underline{H}$CH$_2$), 8.21 (t, 2H, J = 8 Hz, CHN$\underline{H}$). ^{13}C NMR (125 MHz, (CD$_3$)$_2$SO): δ 13.93 ($\underline{C}$H$_3$CH$_2$), 18.29 ($\underline{C}$H$_3$CH), 22.05 ($\underline{C}$H$_2$CH$_3$), 22.48 (CH$_2$), 26.09 (CH$_2$), 27.69 (CH$_2$), 29.05 ($\underline{C}$H$_3$CO), 30.74 (CH$_2$), 30.99 (CH$_2$), 31.76 (CH$_2$), 38.50 (NCH$_2$), 42.36 ($\underline{C}$HCH$_3$), 48.21 ($\underline{C}$HCH$_2$), 52.17 (CH$_2$OH), 58.43 (NCH$_2$), 66.84 (OCH$_2$), 113.97 (CHCH$\underline{C}$H), 114.62 ($\underline{C}$HCHCH), 120.88 (C$\underline{C}$HC), 130.33 (CH$\underline{C}$HCH), 144.00 (N$\underline{C}$CH), 158.41 (NCCH$\underline{C}$), 167.27 (CH$_3$CH$\underline{C}$=O), 168.89 (CH$_2\underline{C}$=O), 171.33 (OCH$_2\underline{C}$=O), 171.88 (CH$_3\underline{C}$=O), 173.25 (NH$_2\underline{C}$=O); MALDI-TOF (*m/z*) Calcd for $C_{27}H_{43}N_5O_7$ [M+Na]$^+$: 572.3060, found: 572.2366.

*4.2.6. (R)-N^1-hexyl-4-((S)-2-(2-(3-(N-(3-hydroxypropyl)butyramido)phenoxy)acetamido) propanamido)pentanediamide (**8**)*

DMF (2 mL) solution of **19** (0.1 g, 0.33 mmol) was mixed to an ice-cooled THF (3 mL) containing 1-hydroxypyrrolidine-2,5-dione, (0.04 g, 0.33 mmol) and **23** (0.1 g, 0.33 mmol). This was followed by the addition of dicyclohexylcarbodiimide (0.07 g, 0.33 mmol). Overnight stirring at room temperature resulted in dicyclohexyl urea precipitates. After filtration, the solvents were removed *in vacuo*. Residue thus obtained was purified over flash silica column (Chloroform/Methanol, 5:1), which gave an air-sensitive compound **8** (0.092 g, 48 %) as white powder. Alternatively, methanol (5 mL) containing **8** (0.05 g, 0.1 mmol) was stirred with butyric anhydride (0.017 ml, 0.1 mmol) at room temperature, which afforded **8** in quantitative yield: R_f = 0.35; ^{1}H NMR (500 MHz, (CD$_3$)$_2$SO): δ 0.73 (t, 3H, J = 7 Hz, C$\underline{H}_3$(CH$_2$)$_2$CO), 0.84 (t, 3H, J = 7 Hz, C$\underline{H}_3$CH$_2$), 1.21 (m, 8H, CH$_3$(C$\underline{H}_2$)$_4$), 1.24 (d, 3H, J = 7 Hz, CHC$\underline{H}_3$), 1.33 (quint., 2H, J = 7

Hz, $CH_3(CH_2)_3C\underline{H_2}$), 1.43 (m, 2H, $CH_3C\underline{H_2}CH_2CO$), 1.52 (quint., 2H, J = 7 Hz, $CH_2C\underline{H_2}CH_2OH$), 1.70 (m, 1H, CHC<u>H</u>H), 1.94 (m, 3H, CHCH<u>H,</u> C<u>H</u>$_2$OH), 2.05 (t, 2H, J = 7 Hz, $CHCH_2C\underline{H_2}$), 2.97 (m, 2H, $CONHC\underline{H_2}$), 3.63 (t, 2H, J = 7 Hz, $NHC\underline{H_2}CH_2OH$), 4.10 (td, 1H, J = 5, 8 Hz, C<u>H</u>CH_2), 4.35 (quint., 1H, J = 7 Hz, C<u>H</u>CH_3), 4.41 (s, 1H, OH), 4.56 (dd, 2H, J = 15 Hz, OCH_2), 6.84-6.96 (m, 3H, CH_{Ar}), 7.07 (s, 1H, NH_2), 7.31 (s, 1H, NH_2), 7.35 (t, 1H, J = 8 Hz, CH_{Ar}), 7.79 (t, 1H, J = 5 Hz, N<u>H</u>CH_2), 8.26 (dd, 2H, J = 5 Hz, CHN<u>H</u>). ^{13}C NMR (125 MHz, $(CD_3)_2SO$): δ 13.67 (<u>C</u>$H_3(CH_2)_2CO$), 13.96 (<u>C</u>$H_3(CH_2)_5NH$), 18.32 (<u>C</u>H_3CH), 22.09 (<u>C</u>H_2CH_3), 26.12 (CH_2), 27.73 (CH_2), 29.09 (CH_2), 30.81 (CH_2), 31.03 (CH_2), 31.80 (CH_2), 35.52 (CH_2), 38.52 (NCH_2), 45.88 (NH<u>C</u>H_2), 48.24 (<u>C</u>HCH_3), 52.23 (<u>C</u>HCH_2), 58.47 (CH_2OH), 66.82 (OCH_2), 104.56 (C<u>C</u>HC), 113.94 (<u>C</u>H_2CONH), 114.83 (<u>C</u>HCHCH), 121.14 (CHCH<u>C</u>H), 130.37 (CH<u>C</u>HCH), 143.63 (N<u>C</u>CH), 158.46 (NCCH<u>C</u>), 167.26 ($CH_3CH\underline{C}$=O), 171.25 ($CH_3(CH_2)_2\underline{C}$=O), 171.33 ($CH_2\underline{C}$=O), 171.90 ($OCH_2\underline{C}$=O), 173.28 ($NH_2\underline{C}$=O); MALDI-TOF (*m/z*) Calcd for $C_{29}H_{47}N_5O_7$ $[M+Na]^+$: 600.3373, found: 600.2922.

*4.2.7. tert-butyl 2-(3-((2-hydroxyethyl)amino)phenoxy)acetate (**10**)*

2-bromoethanol (0.13g, 1.08 mmol) was added dropwise (45 minutes) in refluxing ethanol (10 ml) containing **10** (0.2 g, 0.9 mmol) and Hünig's base (0.19 ml, 1.08 mmol). The reaction was stopped after 8 hours, and the solvent was removed *in vacuo*. The residue was then purified by silica gel column chromatography, which afforded **10** (0.14g, 58%) as brown syrup: R_f = 0.51 (EtOAc/Hexane, 3:2); ^{1}H NMR (500 MHz, $CDCl_3$): δ 1.49 (s, 9H, $C(CH_3)_3$), 3.28 (t, 2H, J = 5 Hz, CH_2), 3.82 (t, 2H, J = 5 Hz, CH_2), 4.47 (s, 2H, CH_2), 6.22-6.25 (m, 2H, CH_{Ar}), 6.28 (dd, 1H, J = 2, 8 Hz, CH_{Ar}), 7.07 (t, 1H, J = 8 Hz, CH_{Ar}). ^{13}C NMR (125 MHz, $CDCl_3$): δ 28.03 ($C(\underline{C}H_3)_3$), 45.99 (<u>C</u>H_2NH), 61.16 (<u>C</u>H_2OH), 65.58 (O<u>C</u>H_2), 82.22 (<u>C</u>$(CH_3)_3$), 100.04 (CH),

103.01 (CH), 107.31 (CH), 129.98 (CH), 149.51 (CCH), 159.15 (CCH), 168.21 (C=O); MALDI-TOF (*m/z*) Calcd for $C_{14}H_{21}NO_4$ $[M+H]^+$: 268.1549, found: 268.1540.

*4.2.8. tert-butyl 2-(3-(N-(2-hydroxyethyl)acetamido)phenoxy)acetate (**12**)*

Acetic anhydride (0.04 ml, 0.44 mmol) was added dropwise (25 minutes) in methanol (5 ml) containing **10** (0.1 g, 0.37 mmol). The reaction was monitored by TLC for the consumption of **10**. Solvent was then removal by rotary evaporator, which afforded **12** (0.115 g, >99 %) as brown syrup: Rf = 0.61 (ethyl acetate); ^{1}H NMR (500 MHz, $CDCl_3$): δ 1.49 (s, 9H, $C(CH_3)_3$), 1.89 (s, 3H, CH_3CO), 3.77 (t, 2H, J = 5 Hz, CH_2), 3.86 (t, 2H, J = 5 Hz, CH_2), 4.50 (s, 2H, CH_2), 6.76 (t, 1H, J = 2 Hz, CH_{Ar}), 6.84 (m, 1H, CH_{Ar}), 6.88 (dd, 1H, J = 2, 8 Hz, CH_{Ar}), 7.34 (t, 1H, J = 8 Hz, CH_{Ar}). ^{13}C NMR (125 MHz, $CDCl_3$): δ 22.57 (CH_3CO), 28.02 ($C(CH_3)_3$), 52.80 (CH_2N), 61.87 (CH_2OH), 65.56 (OCH_2), 82.74 ($C(CH_3)_3$), 114.18 (CH), 114.33 (CH), 120.77 (CH), 130.68 (CH), 144.37 (CCH), 158.88 (CCH), 167.48 (C=O), 172.80 (C=O); EI-MS (m/z) Calcd for C16H23NO5 [M+H]: 310.1654, found: 310.1649

*4.2.9. tert-butyl 2-(3-(N-(3-hydroxypropyl)acetamido)phenoxy)acetate (**13**)*

Acetic anhydride (0.04 ml, 0.42 mmol) was added dropwise (25 minutes) in methanol (5 ml) containing **11** (0.1 g, 0.35 mmol). The reaction was monitored by TLC for the consumption of **11**. Solvent was then removal by rotary evaporator, which afforded **13** (0.115 g, >99 %) as brown syrup: Rf = 0.37 (ethyl acetate/hexane, 1:4); ^{1}H NMR (500 MHz, $CDCl_3$): δ 1.49 (s, 9H, $C(CH_3)_3$), 1.64 (quint, 2H, J = 6 Hz, CH_2), 1.88 (s, 3H, CH_3CO), 3.62 (t, 2H, J = 6 Hz, CH_2), 3.84 (t, 2H, J = 6 Hz, CH_2), 4.52 (s, 2H, CH_2), 6.69 (t, 1H, J = 2 Hz, CH_{Ar}), 6.76 (dd, 1H, J = 2, 8 Hz, CH_{Ar}), 6.87 (dd, 1H, J = 2, 8 Hz, CH_{Ar}), 7.34 (t, 1H, J = 8 Hz, CH_{Ar}). ^{13}C NMR (125 MHz,

$CDCl_3$): δ 22.37 (CH_3CO), 28.00 ($C(\underline{C}H_3)_3$), 30.05 (CH_2), 45.48 ($\underline{C}H_2N$), 58.15 ($\underline{C}H_2OH$), 65.59 ($O\underline{C}H_2$), 82.74 ($\underline{C}(CH_3)_3$), 113.88 (CH), 114.66 (CH), 120.84 (CH), 130.66 (CH), 143.70 (CCH), 158.89 (CCH), 167.44 (C=O), 171.90 (C=O); EI-MS (m/z) Calcd for $C_{17}H_{25}NO_5$ [M+H]: 324.1811, found: 324.1805.

*4.2.10. tert-butyl 2-(3-(N-(2-hydroxyethyl)butyramido)phenoxy)acetate (**14**)*

Butyric anhydride (0.07 ml, 0.45 mmol) was added dropwise (25 minutes) in methanol (5 ml) containing **10** (0.1 g, 0.37 mmol). The reaction was monitored by TLC for the consumption of **10**. Solvent was then removal by rotary evaporator, which afforded **14** (0.125 g, >99 %) as brown syrup: Rf = 0.64 (ethyl acetate/hexane, 2:3); ^{1}H NMR (500 MHz, $CDCl_3$): δ 0.83 (t, 3H, J = 7 Hz, $C\underline{H}_3CH_2$), 1.49 (s, 9H, $C(CH_3)_3$), 1.59 (m, 2H, $CH_3C\underline{H}_2$), 2.07 (t, 2H, J = 7 Hz, $C\underline{H}_2CO$), 3.23 (s, 1H, OH), 3.76 (m, 2H, CH_2), 3.86 (t, 2H, J = 5 Hz, CH_2), 4.53 (s, 2H, CH_2), 6.74 (t, 1H, J = 2 Hz, CH_{Ar}), 6.83 (dd, 1H, J = 2, 7 Hz, CH_{Ar}), 6.88 (dd, 1H, J = 2, 8 Hz, CH_{Ar}), 7.33 (t, 1H, J = 8 Hz, CH_{Ar}). ^{13}C NMR (125 MHz, $CDCl_3$): δ 13.58 ($\underline{C}H_3CH_2$), 18.62 ($CH_3C\underline{H}_2$), 27.85 ($C(\underline{C}H_3)_3$), 36.00 ($CH_3CH_2C\underline{H}_2CO$), 52.36 ($\underline{C}H_2N$), 61.10 ($\underline{C}H_2OH$), 65.41 ($O\underline{C}H_2$), 82.52 ($\underline{C}(CH_3)_3$), 113.98 (CH), 114.44 (CH), 120.96 (CH), 130.43 (CH), 143.78 (CCH), 158.68 (CCH), 167.41 (C=O), 174.90 (C=O); EI-MS (m/z) Calcd for $C_{18}H_{27}NO_5$ [M+H]: 338.1967, found: 338.1962.

*4.2.11. tert-butyl 2-(3-(N-(3-hydroxypropyl)butyramido)phenoxy)acetate (**15**)*

Butyric anhydride (0.07 ml, 0.42 mmol) was added dropwise (25 minutes) in methanol (5 ml) containing **11** (0.1 g, 0.35 mmol). The reaction was monitored by TLC for the consumption of **11**. Solvent was then removal by rotary evaporator, which afforded **15** (0.125 g, >99 %) as

brown syrup: Rf = 0.42 (hexane/ethyl acetate, 2:3); ^{1}H NMR (500 MHz, $CDCl_3$): δ 0.82 (t, 3H, J = 7 Hz, $C\underline{H}_3CH_2$), 1.48 (s, 9H, $C(CH_3)_3$), 1.55-1.64 (m, 4H, $(CH_2)_2$), 2.05 (t, 2H, J = 8 Hz, $CH_3CH_2C\underline{H}_2$), 3.60 (m, 2H, CH_2), 3.83 (t, 2H, J = 5 Hz, CH_2), 3.99 (s, 1H, OH), 4.52 (s, 2H, CH_2), 6.66 (m, 1H, CH_{Ar}), 6.74 (dd, 1H, J = 2, 8 Hz, CH_{Ar}), 6.86 (dd, 1H, J = 2, 8 Hz, CH_{Ar}), 7.33 (t, 1H, J = 8 Hz, CH_{Ar}). ^{13}C NMR (125 MHz, $CDCl_3$): δ 13.55 ($\underline{C}H_3CH_2$), 18.68 ($CH_3\underline{C}H_2$), 27.81 ($C(\underline{C}H_3)_3$), 29.90 (CH_2), 35.77 (CH_2), 45.41 ($\underline{C}H_2N$), 58.00 ($\underline{C}H_2OH$), 65.39 ($O\underline{C}H_2$), 82.51 ($\underline{C}(CH_3)_3$), 113.66 (CH), 114.69 (CH), 120.93 (CH), 130.44 (CH), 143.18 ($\underline{C}CH$), 158.68 ($\underline{C}CH$), 167.33 (C=O), 174.21 (C=O); EI-MS (m/z) Calcd for $C_{19}H_{29}NO_5$ [M+H]: 352.2124, found: 352.2118.

4.2.12. 2-(3-(*N*-(2-hydroxyethyl)acetamido)phenoxy)acetic acid ***(16)***

Aqueous NaOH (0.5 N, 2 ml) was carefully added to an ice-cooled solution of **12** (0.1 g, 0.32 mmol) in dioxane (3 mL). Hydrolysis was monitored with TLC until consumption of all the starting material. Reaction mixture was neutralized with dilute HCl (0.5 N) to give **16** (0.053 g, >99%): R_f = 0.24 ($CHCl_3/CH_3OH$, 2:3); ^{1}H NMR (500 MHz, $(CD_3)_2SO$): δ 1.62, 1.72 (s, 3H, CH_3CO), 3.02, 3.43 (q, 2H, J = 6 Hz, NCH_2), 3.53, 3.61 (t, 2H, J = 6 Hz, $\underline{CH_2}OH$), 4.01, 4.13 (s, 2H, OCH_2), 4.78 (br, 1H, OH), 5.41 (t, 1H, OH), 6.01-6.10, 6.78 (m, 3H, CH), 6.87, 7.26 (t, 1H, J = 8 Hz, CH); ^{13}C NMR (125 MHz, $(CD_3)_2SO$): δ 22.52, 40.42 ($\underline{CH_3}CO$), 45.67, 50.73 (CH_2), 57.90, 59.61 (CH_2), 67.39, 67.80 (CH_2), 98.55, 113.61 (CH_{Ar}), 102.04, 114.58 (CH_{Ar}), 104.61, 119.31 (CH_{Ar}), 129.16, 129.69 (CH_{Ar}), 144.07, 150.07 (C_{Ar}), 159.66, 159.90 (C_{Ar}), 169.10 (CO), 171.04, 172.01 (CO); EI-MS (m/z) Calcd for $C_{12}H_{15}NO_5$ [M+Na]: 276.0848, found: 276.0843.

*4.2.13. 2-(3-(N-(3-hydroxypropyl)acetamido)phenoxy)acetic acid (**17**)*

Aqueous NaOH (0.5 N, 2 ml) was carefully added to an ice-cooled solution of **13** (0.1 g, 0.31 mmol) in dioxane (3 mL). Hydrolysis was monitored with TLC until consumption of all the starting material. Reaction mixture was neutralized with dilute HCl (0.5 N) to give **17** (0.053 g, 65%); R_f = 0.23 (CH_2Cl_2/CH_3OH, 5:1); ^{1}H NMR (500 MHz, $(CD_3)_2SO$): δ 1.22, 1.72 (s, 3H, CH_3CO), 1.54, 1.67 (quint. 2H, J = 7 Hz, $NCH_2\underline{CH_2}$), 3.00, 3.47 (t, 2H, J = 7 Hz, NCH_2), 3.36, 3.61 (t, 2H, J = 7 Hz, $\underline{CH_2}OH$), 4.18, 4.27 (s, 2H, OCH_2), 4.49, 5.45 (br, 1H, OH), 6.01, 6.76 (dd, 1H, J = 2, 8 Hz, CH), 6.05, 6.73 (s, 1H, CH), 6.10, 6.81 (dd, 1H, J = 2, 8 Hz, CH), 6.88, 7.28 (t, 1H, J = 8 Hz, CH); ^{13}C NMR (125 MHz, $(CD_3)_2SO$): δ 22.05, 22.46 ($\underline{CH_3}CO$), 30.75, 31.95 (CH_2), 40.09, 45.68 (CH_2), 58.39, 58.66 (CH_2), 66.76, 67.36 (CH_2), 98.33, 114.53 (CH_{Ar}), 101.63, 119.60 (CH_{Ar}), 104.87, 129.18 (CH_{Ar}), 113.61, 129.89 (CH_{Ar}), 143.71, 159.45 (C_{Ar}), 150.27, 159.60 (C_{Ar}), 168.89 (CO), 171.67, 172.39 (CO); EI-MS (m/z) Calcd for $C_{13}H_{17}NO_5$ [M+H]: 268.1185, found: 268.1179.

*4.2.14. 2-(3-(N-(2-hydroxyethyl)butyramido)phenoxy)acetic acid (**18**)*

Aqueous NaOH (0.5 N, 2 ml) was carefully added to an ice-cooled solution of **14** (0.1 g, 0.3 mmol) in dioxane (3 mL). Hydrolysis was monitored with TLC until consumption of all the starting material. Reaction mixture was neutralized with dilute HCl (0.5 N) to give **18** (0.083 g, >99%): R_f = 0.25 (CH_2Cl_2/CH_3OH, 5:1); ^{1}H NMR (400 MHz, $(CD_3)_2SO$): δ 0.81 (t, 3H, J = 7 Hz, $C\underline{H_3}CH_2$), 1.51 (m, 2H, $CH_3C\underline{H_2}$), 2.01 (t, 2H, J = 7 Hz, $C\underline{H_2}CO$), 3.60 (m, 2H, CH_2), 3.71 (t, 2H, J = 5 Hz, CH_2), 4.40 (s, 2H, CH_2), 6.60 (t, 1H, J = 2 Hz, CH_{Ar}), 6.71 (dd, 1H, J = 2, 7 Hz, CH_{Ar}), 6.71 (dd, 1H, J = 2, 8 Hz, CH_{Ar}), 7.21 (t, 1H, J = 8 Hz, CH_{Ar}); ^{13}C NMR (100 MHz, $(CD_3)_2SO$): δ 13.65 ($\underline{CH_3}$), 18.28 ($CH_3\underline{CH_2}$), 35.48 (CH_2), 50.85 (CH_2), 57.98 (CH_2), 67.65 (CH_2), 113.50 (CH_{Ar}), 114.94 (CH_{Ar}), 119.80 (CH_{Ar}), 129.79 (CH_{Ar}), 143.70 (C_{Ar}), 159.53 (C_{Ar}),

171.53 (CO), 171.68 (CO); EI-MS (m/z) Calcd for $C_{14}H_{19}NO_5$ [M+H]: 282.1341, found: 282.1336.

*4.2.15. 2-(3-(N-(3-hydroxypropyl)butyramido)phenoxy)acetic acid (**19**)*

Aqueous NaOH (0.5 N, 2 ml) was carefully added to an ice-cooled solution of **15** (0.1 g, 0.28 mmol) in dioxane (3 mL). Hydrolysis was monitored with TLC until consumption of all the starting material. Reaction mixture was neutralized with dilute HCl (0.5N) to give **19** (0.084 g, >99%): R_f = 0.22 (CH_2Cl_2/CH_3OH, 5:1); ^{1}H NMR (400 MHz, $(CD_3)_2SO$): δ 0.79 (t, 3H, J = 7 Hz, $C\underline{H}_3CH_2$), 1.51-1.65 (m, 4H, $(CH_2)_2$), 2.01 (t, 2H, J = 8 Hz, $CH_3CH_2C\underline{H}_2$), 3.71 (m, 2H, CH_2), 3.73 (t, 2H, J = 5 Hz, CH_2), 4.50 (s, 2H, CH_2), 6.51 (m, 1H, CH), 6.64 (dd, 1H, J = 2, 8 Hz, CH), 6.63 (dd, 1H, J = 2, 8 Hz, CH), 7.13 (t, 1H, J = 8 Hz, CH); ^{13}C NMR (100 MHz, $(CD_3)_2SO$): δ 13.62 ($\underline{CH}_3$), 18.30 ($CH_3\underline{CH}_2$), 30.80 (CH_2), 35.42 (CH_2), 45.82 (CH_2), 58.42 (CH_2), 67.72 (CH_2), 113.54 (CH_{Ar}), 114.79 (CH_{Ar}), 119.65 (CH_{Ar}), 129.84 (CH_{Ar}), 143.29 (C_{Ar}), 159.69 (CO), 171.26 (CO); EI-MS (m/z) Calcd for $C_{15}H_{21}NO_5$ [M+H]: 296.1498, found: 296.1492.

*4.2.16. 2-(3-((2-hydroxyethyl)amino)phenoxy)acetic acid (**20**)*

Aqueous NaOH (0.5 N, 2 ml) was carefully added to an ice-cooled solution of **10** (0.1 g, 0.37 mmol) in dioxane (3 mL). Hydrolysis was monitored with TLC until consumption of all the starting material. Reaction mixture was neutralized with dilute HCl (0.5 N) to give **21** (0.079 g, >99%): R_f = 0.26 (CH_2Cl_2/CH_3OH, 5:1); ^{1}H NMR (400 MHz, $CDCl_3$): δ 3.19 (t, 2H, J = 7 Hz, $NH\underline{CH_2}$), 3.69 (t, 2H, J = 7 Hz, $\underline{CH_2}OH$), 4.33 (s, 2H, OCH_2), 6.23 (m, 3H, CH), 6.97 (t, 1H, $C\underline{CH}C$). ^{13}C NMR (100 MHz, $CDCl_3$): δ 48.93 ($NHCH_2$), 62.57 (CH_2OH), 69.40 (OCH_2),

103.49 (CH), 107.41 (CH), 110.61 (CH), 133.07 (CH), 152.24 (CCH), 161.64 (CCH), 179.61 (CO). MALDI-TOF (*m/z*) Calcd for $C_{10}H_{13}NO_4$ $[M+Na]^+$: 234.0742, found: 234.1124.

*4.2.17. tert-butyl 2-(3-(bis(2-hydroxyethyl)amino)phenoxy)acetate (**21**)*

2-bromoethanol (0.11 ml, 1.5 mmol) was added dropwise (45 minutes) in refluxing ethanol (10 ml) containing **11** (0.2 g, 0.75 mmol) and Hünig's base (0.26 ml, 1.5 mmol). The reaction was stopped after overnight reflux, and the solvent removed under reduced pressure. Silica column was then used to purify the residue, which afforded **23** (0.165 g, 71%) as brown syrup: Rf = 0.39 (ethyl acetate/hexane, 4:1), ^{1}H NMR (500 MHz, $CDCl_3$): δ 1.49 (s, 9H, $C(CH_3)_3$), 3.57 (t, 4H, J = 5 Hz, NCH_2), 3.86 (t, 4H, J = 5 Hz, CH_2), 4.48 (s, 2H, CH_2), 6.21 (dd, 1H, J = 2, 8 Hz, CH), 6.30 (t, 1H, J = 2 Hz, CH), 6.34 (dd, 1H, J = 2, 8 Hz, CH), 7.12 (t, 1H, J = 8 Hz, CH). ^{13}C NMR (125 MHz, $CDCl_3$): δ 28.07 ($C(CH_3)_3$), 55.44 (NCH_2), 60.90 $(CH_2OH)_2$, 65.72 (OCH_2), 82.31 ($C(CH_3)_3$), 100.30 (CH), 101.66 (CH), 106.56 (CH), 129.96 (CH), 149.27 (CCH), 159.12 (CCH), 168.26 (C=O); MALDI-TOF (*m/z*) Calcd for $C_{16}H_{25}NO_5$ $[M+K]^+$: 350.1370, found: 350.1446.

*4.2.18. 2-(3-(bis(2-hydroxyethyl)amino)phenoxy)acetic acid (**22**)*

Aqueous NaOH (0.5 N, 2 ml) was carefully added to an ice-cooled solution of **21** (0.1 g, 0.32 mmol) in dioxane (3 mL). Hydrolysis was monitored with TLC until consumption of all the starting material. Reaction mixture was neutralized with dilute HCl (0.5N) to give **25** (0.082 g, >99%): R_f = 0.20 (CH_2Cl_2/CH_3OH, 4:1); ^{1}H NMR (400 MHz, D_2O): δ 3.59 (t, 4H, J = 5 Hz, NCH_2), 3.75 (t, 4H, J = 5 Hz, CH_2OH), 4.77 (s, 2H, OCH_2), 7.13 (m, 3H, CH), 7.52 (t, 1H, J = 2 Hz, CH). ^{13}C NMR (100 MHz, D_2O): δ 58.00 (CH_2OH), 62.50 (NCH_2), 68.12 (OCH_2), 111.56

(CH), 118.03 (CH), 119.08 (CH), 134.36 (CCH), 134.46 (CH), 161.36 (CCH), 176.06 (CO). MALDI-TOF (*m/z*) Calcd for $C_{12}H_{17}NO_5$ $[M+H]^+$: 256.1185, found: 256.0930.

4.3. Cell maintenance

ATCC (American Type Culture Collection) supplied THP-1 cells. The monocytes were maintained in CO_2 atmosphere (5%) at 37 °C by using the fetal bovine serum (10%, heat inactivated) containing RPMI-1640 medium. Antimycotic 100x antibiotic (1%) was also added to the medium. Hemocytometer was used to perform the cell counting and trypan blue cellular exclusion method was used to determine the cell viability.

4.4. ICAM-1 induction in THP-1 cells

0.5 x 10^6 monocytes per well were incubated for 24 hours. Then, 20 µM of each DMP was used to incubate monocytes for the next 21 hours. Alternatively, monocytes were initially treated for 1 hour with amphiphilic DMPs at different concentrations (0.1–32 µM) followed by LPS (0.1 µg/mL) stimulation for the next 20 hours. The cells were isolated by centrifugation (5 min, 1000xg), and then washed with PBS. For FACS analysis, they were re-suspended in bovine serum albumen (0.1%) containing PBS (100 µL).

4.5. ICAM-1 induction in THP-1 macrophages

To induce differentiation, 0.5 x 10^6 monocytes were plated in fetal bovine serum (10%) containing RPMI-1640 with PMA (20 ng/mL). The medium was removed after 48 hours, and PBS was employed to wash the macrophages. Serum-free RPMI-1640 medium was used to refill the wells, and the macrophages were then stimulated with 20 µM DMPs. For the positive control, 20 µM of murabutide was used. Serum-free medium was then used to refill the wells. For

combinatory synergistic studies, macrophages were first stimulated for 1 hour with 0.1–64 µM of DMP **6**, and then 0.1 µg/mL of LPS was added for the next 20 hours. PBS was used to wash the macrophages via centrifugation (4 minutes, 400 xg). Overall cell viability was determined by subtracting trypan blue-positive dead cells found in the washings. For FACS analysis, gentle cold shocks were given to detach the macrophages, which were then suspended in 100 µL PBS with 0.1% bovine serum albumin. Immunostaining with phycoerythrin-conjugated monoclonal antibody specific to CD54 (BD Biosciences, USA) was used to determine ICAM-1 expression. Briefly, macrophages were incubated with the antibody at 4 °C in the dark for 1 hour. After two washings, macrophages were suspended in PBS (500 µL). Flow cytometry of the sample was done by acquiring 20,000 events using BD FACSCalibur™ instrument and CELLQUEST PRO™ software. ICAM-1 expression was determined as mean fluorescence intensity (MFI) on the FL2 channel.

4.6. Cytokine induction and measurement

To induce differentiation, 0.5 x 10^6 monocytes were plated in RPMI-1640 and PMA (20 ng/mL) containing wells. The medium was removed after 48 hours followed by PBS washing as described above. Macrophages were incubated for three hours in serum-free medium followed by their exposure to stimuli for 24 hours. Culture supernatants were stored at -80 °C until tested. Maxisorp 96-well plates were used to perform enzyme-linked immunosorbent assay (ELISA). The cytokine (TNF-α) was quantified using eBiosciences® ELISA kits (Ready-Set-Go!). BMG Labtech micro-plate reader was employed to measure the absorbance at 450 nm, while the wavelength correction was set at 540 nm. Cytokine values were determined using a standard

curve, which was generated with 2nd order polynomial regression analysis, and the results were presented as mean of two separate experiments ± SEM.

4.7. Statistical Analyses

GraphPad Prism™ software was used for one-way ANOVA statistical analyses. The results were shown as mean ± SEM and $p < 0.05$ was regarded statistically significant.

4.8. Computational Studies

The automated docking program MOE-Dock 2018.01[72] was used for docking of DMPs into the binding cavity of NOD2. The receptor was prepared, and the energy was minimized by using Amber10 force-field. The compounds were built using MOE-builder module implemented in MOE followed by energy-minimization with MMFF94x partial charges [73] and converted into mol2 format. Further, all the compounds were docked into the binding pocket using default docking protocol. For human NOD2 receptor, the previous literature data indicates that putative binding is based on residues Gly879. Thr899, Trp907, Val935, Glu959, Lys989, and Ser991 [74]. The residues Gly879 and Trp907 are conserved in both human and rabbit NOD2 receptors. The binding site of NOD2-LRR comprises of concave shaped β sheets, whereas the α helices are folded into convex region [73] as illustrated in Figure 7. The poses were ranked according to the MOE score (Table 2). The best pose was selected for each compound and then analyzed for protein ligand interactions.

Acknowledgement

Lakehead University and Natural Sciences and Engineering Research Council of Canada (NSERC, Grant EGP 469917-14 and RGPIN 2017-05363) supported this work.

Supporting Information

Additional data relevant to this paper can be found in supporting information file.

References

[1] R. Medzhitov, C. Janeway, Innate Immunity, N. Engl. J. Med. 343 (2000) 338–344. https://doi.org/10.1056/NEJM200008033430506.

[2] A. Iwasaki, R. Medzhitov, Control of adaptive immunity by the innate immune system, Nat. Immunol. 16 (2015) 343–353. https://doi.org/10.1038/ni.3123.

[3] S. Tartey, O. Takeuchi, Pathogen recognition and Toll-like receptor targeted therapeutics in innate immune cells, Int. Rev. Immunol. 36 (2017) 57–73. https://doi.org/10.1080/08830185.2016.1261318.

[4] L.E. Reddick, N.M. Alto, Bacteria Fighting Back: How Pathogens Target and Subvert the Host Innate Immune System, Mol. Cell. 54 (2014) 321–328. https://doi.org/10.1016/j.molcel.2014.03.010.

[5] S.E. Girardin, I.G. Boneca, J. Viala, M. Chamaillard, A. Labigne, G. Thomas, D.J. Philpott, P.J. Sansonetti, Nod2 Is a General Sensor of Peptidoglycan through Muramyl Dipeptide (MDP) Detection, J. Biol. Chem. 278 (2003) 8869–8872. https://doi.org/10.1074/jbc.C200651200.

[6] W. Strober, P.J. Murray, A. Kitani, T. Watanabe, Signalling pathways and molecular interactions of NOD1 and NOD2, Nat. Rev. Immunol. 6 (2006) 9–20. https://doi.org/10.1038/nri1747.

[7] J.D. Van Buul, M. Fernandez-Borja, E.C. Anthony, P.L. Hordijk, Expression and Localization of NOX2 and NOX4 in Primary Human Endothelial Cells, Antioxid. Redox Signal. 7 (2005) 308–317. https://doi.org/10.1089/ars.2005.7.308.

[8] F. Ellouz, A. Adam, R. Ciorbaru, E. Lederer, Minimal structural requirements for adjuvant activity of bacterial peptidoglycan derivatives, Biochem. Biophys. Res. Commun. 59 (1974) 1317–1325. https://doi.org/10.1016/0006-291X(74)90458-6.

[9] A. Malabarba, T.I. Nicas, R. Ciabatti, Glycopeptide resistance in multiple antibiotic-resistant Gram-positive bacteria: a current challenge for novel semi-synthetic glycopeptide derivatives, Eur. J. Med. Chem. 32 (1997) 459–478. https://doi.org/10.1016/S0223-5234(97)84010-X.

[10] C.L. Grimes, L.D.Z. Ariyananda, J.E. Melnyk, E.K. O'Shea, The Innate Immune Protein Nod2 Binds Directly to MDP, a Bacterial Cell Wall Fragment, J. Am. Chem. Soc. 134 (2012) 13535–13537. https://doi.org/10.1021/ja303883c.

[11] C. Ogawa, Y.-J. Liu, K. S. Kobayashi, Muramyl Dipeptide and its Derivatives: Peptide Adjuvant in Immunological Disorders and Cancer Therapy, Curr. Bioact. Compd. 7 (2011) 180–197. https://doi.org/10.2174/157340711796817913.

[12] Z. Jakopin, Murabutide Revisited: A Review of its Pleiotropic Biological Effects, Curr. Med. Chem. 20 (2013) 2068–2079. https://doi.org/10.2174/0929867311320160002.

[13] N. Zhao, Y. Ma, S. Zhang, X. Fang, Z. Liang, G. Liu, New muramyl dipeptide (MDP) mimics without the carbohydrate moiety as potential adjuvant candidates for a therapeutic hepatitis B vaccine (HBV), Bioorg. Med. Chem. Lett. 21 (2011) 4292–4295. https://doi.org/10.1016/j.bmcl.2011.05.056.

[14] O. Lockhoff, Glycolipids as Immunomodulators: Syntheses and Properties, Angew. Chemie Int. Ed. English. 30 (1991) 1611–1620. https://doi.org/10.1002/anie.199116111.

[15] L.A. Chedid, M.A. Parant, F.M. Audibert, G.J. Riveau, F.J. Parant, E. Lederer, J.P. Choay, P.L.

Lefrancier, Biological activity of a new synthetic muramyl peptide adjuvant devoid of pyrogenicity., Infect. Immun. 35 (1982) 417–24. http://www.ncbi.nlm.nih.gov/pubmed/7035362.

[16] P. Lefrancier, E. Lederer, Muramyl-peptides, Pure Appl. Chem. 59 (1987) 449–454. https://doi.org/10.1351/pac198759030449.

[17] K. Dzierzbicka, A. Wardowska, P. Trzonkowski, Recent Developments in the Synthesis and Biological Activity of Muramylpeptides, Curr. Med. Chem. 18 (2011) 2438–2451. https://doi.org/10.2174/092986711795843173.

[18] S. Wang, J. Yang, X. Li, Z. Liu, Y. Wu, G. Si, Y. Tao, N. Zhao, X. Hu, Y. Ma, G. Liu, Discovery of 1,4-Benzodiazepine-2,5-dione (BZD) Derivatives as Dual Nucleotide Binding Oligomerization Domain Containing 1/2 (NOD1/NOD2) Antagonists Sensitizing Paclitaxel (PTX) To Suppress Lewis Lung Carcinoma (LLC) Growth in Vivo, J. Med. Chem. 60 (2017) 5162–5192. https://doi.org/10.1021/acs.jmedchem.7b00608.

[19] K. Biteau, R. Guiho, M. Chatelais, J. Taurelle, J. Chesneau, N. Corradini, D. Heymann, F. Redini, L-MTP-PE and zoledronic acid combination in osteosarcoma: preclinical evidence of positive therapeutic combination for clinical transfer., Am. J. Cancer Res. 6 (2016) 677–89. http://www.ncbi.nlm.nih.gov/pubmed/27152244.

[20] B. Guy, The perfect mix: recent progress in adjuvant research, Nat. Rev. Microbiol. 5 (2007) 396–397. https://doi.org/10.1038/nrmicro1681.

[21] W. Keitel, R. Couch, N. Bond, S. Adair, G. Van Nest, C. Dekker, Pilot evaluation of influenza virus vaccine (IVV) combined with adjuvant, Vaccine. 11 (1993) 909–913. https://doi.org/10.1016/0264-410X(93)90376-9.

[22] J. Wintsch, C.-L. Chaignat, D.G. Braun, M. Jeannet, H. Stalder, S. Abrignani, D. Montagna, F. Clavijo, P. Moret, J.-M. Dayer, T. Staehelin, B. Doe, K.S. Steimer, D. Dina, A. Cruchaud, Safety and Immunogenicity of a Genetically Engineered Human Immunodeficiency Virus Vaccine, J. Infect. Dis. 163 (1991) 219–225. https://doi.org/10.1093/infdis/163.2.219.

[23] J.O. Kahn, F. Sinangil, J. Baenziger, N. Murcar, D. Wynne, R.L. Coleman, K.S. Steimer, C.L. Dekker, D. Chernoff, Clinical And Immunologic Responses To Human Immunodeficiency Virus (HIV) Type LSF2 gp120 Subunit Vaccine Combined With MF59 Adjuvant With Or Without Muramyl Tripeptide Dipalmitoyl Phosphatidylethanolamine In Non-HIV-Infected Human Volunteers, J. Infect. Dis. 170 (1994) 1288–1291. https://doi.org/10.1093/infdis/170.5.1288.

[24] L. Sanchez-Pescador, R.L. Burke, G. Ott, G. Van Nest, The effect of adjuvants on the efficacy of a recombinant herpes simplex virus glycoprotein vaccine., J. Immunol. 141 (1988) 1720–7. http://www.ncbi.nlm.nih.gov/pubmed/2842401.

[25] N.E. Byars, A.C. Allison, M.W. Harmon, A.P. Kendal, Enhancement of antibody responses to influenza B virus haemagglutinin by use of a new adjuvant formulation, Vaccine. 8 (1990) 49–56. https://doi.org/10.1016/0264-410X(90)90177-N.

[26] S. Zolla□Pazner, C. Alving, R. Belshe, P. Berman, S. Burda, P. Chigurupati, M. Lou Clements, A. Duliege, J. Excler, C. Hioe, J. Kahn, M.J. McElrath, S. Sharpe, F. Sinangil, K. Steimer, M.C. Walker, N. Wassef, S. Xu, Neutralization of a Clade B Primary Isolate by Sera from Human Immunodeficiency Virus—Uninfected Recipients of Candidate AIDS Vaccines, J. Infect. Dis. 175 (1997) 764–774. https://doi.org/10.1086/513969.

[27] N.E. Byars, G. Nakano, M. Welch, D. Lehman, A.C. Allison, Improvement of hepatitis B vaccine

by the use of a new adjuvant, Vaccine. 9 (1991) 309–318. https://doi.org/10.1016/0264-410X(91)90056-C.

[28] A.M. Palache, W.E.P. Beyer, E. Hendriksen, L. Gerez, R. Aston, P.W. Ledger, V. de Regt, R. Kerstens, P.H. Rothbarth, A.D.M.E. Osterhaus, Adjuvancy and reactogenicity of N-acetylglucosaminyl-N-acetylmuramyl-dipeptide (GMDP) orally administered just prior to trivalent influenza subunit vaccine. A double-blind placebo-controlled study in nursing home residents, Vaccine. 14 (1996) 1327–1330. https://doi.org/10.1016/S0264-410X(96)00075-8.

[29] R. Bomford, M. Stapelton, S. Winsor, A. McKnight, T. Andronova, The Control of the Antibody Isotype Response to Recombinant Human Immunodeficiency Virus gp120 Antigen by Adjuvants, AIDS Res. Hum. Retroviruses. 8 (1992) 1765–1771. https://doi.org/10.1089/aid.1992.8.1765.

[30] M. Tsujimoto, S. Kotani, T. Okunaga, T. Kubo, H. Takada, T. Kubo, T. Shiba, S. Kusumoto, T. Takahashi, Y. Goto, F. Kinoshita, Enhancement of humoral immune responses against viral vaccines by a non-pyrogenic 6-O-acyl-muramyldipeptide and synthetic low toxicity analogues of lipid A, Vaccine. 7 (1989) 39–48. https://doi.org/10.1016/0264-410X(89)90009-1.

[31] K. Nerome, Y. Yoshioka, M. Ishida, K. Okuma, T. Oka, T. Kataoka, A. Inoue, A. Oya, Development of a new type of influenza subunit vaccine made by muramyldipeptide-liposome: enhancement of humoral and cellular immune responses, Vaccine. 8 (1990) 503–509. https://doi.org/10.1016/0264-410X(90)90254-J.

[32] E. Telzak, S.M. Wolff, C.A. Dinarello, T. Conlon, A. El Kholy, G.M. Bahr, J.P. Choay, A. Morin, L. Chedid, Clinical Evaluation of the Immunoadjuvant Murabutide, a Derivative of MDP, Administered with a Tetanus Toxoid Vaccine, J. Infect. Dis. 153 (1986) 628–633. https://doi.org/10.1093/infdis/153.3.628.

[33] F.M. Audibert, G. Przewlocki, C.D. Leclerc, M.E. Jolivet, H.S. Gras-Masse, A.L. Tartar, L.A. Chedid, Enhancement by murabutide of the immune response to natural and synthetic hepatitis B surface antigens., Infect. Immun. 45 (1984) 261–6. http://www.ncbi.nlm.nih.gov/pubmed/6735468.

[34] M. Zaoral, J. Ježek, J. Rotta, Preparation and some biological properties of N-acetylmuramyl-alanyl-D-isoglutamine (MDP) analogues, Collect. Czechoslov. Chem. Commun. 47 (1982) 2989–2995. https://doi.org/10.1135/cccc19822989.

[35] I. Azuma, H. Okumura, I. Saiki, M. Kiso, A. Hasegawa, Y. Tanio, Y. Yamamura, Adjuvant activity of carbohydrate analogs of N-acetylmuramyl-L-alanyl-D-isoglutamine on the induction of delayed-type hypersensitivity to azobenzenearsonate-N-acetyl-L-tyrosine in guinea pigs., Infect. Immun. 33 (1981) 834–9. http://www.ncbi.nlm.nih.gov/pubmed/7287186.

[36] P.L. Durette, C.P. Dorn, A. Friedman, A. Schlabach, Synthesis and immunoadjuvant activities of 2-acetamido-5-O-acetyl-6-O-acyl-2-deoxy-3-O-[(R)-2-propionyl-L-alanyl-D-isoglutamine]-D-glucofuranoses as potential prodrug forms of 6-O-acyl derivatives of N-acetylmuramyl dipeptide, J. Med. Chem. 25 (1982) 1028–1033. https://doi.org/10.1021/jm00351a005.

[37] R. Ribić, R. Stojković, L. Milković, M. Antica, M. Cigler, S. Tomić, Design, synthesis and biological evaluation of immunostimulating mannosylated desmuramyl peptides, Beilstein J. Org. Chem. 15 (2019) 1805–1814. https://doi.org/10.3762/bjoc.15.174.

[38] M.A. Parant, F.M. Audibert, L.A. Chedid, M.R. Level, P.L. Lefrancier, J.P. Choay, E. Lederer, Immunostimulant activities of a lipophilic muramyl dipeptide derivative and of desmuramyl peptidolipid analogs., Infect. Immun. 27 (1980) 826–31.

http://www.ncbi.nlm.nih.gov/pubmed/7380554.

[39] R. Ribić, M. Paurević, S. Tomić, Advances in Desmuramyl Peptide Research, Croat. Chem. Acta. 92 (2019) 153–161. https://doi.org/10.5562/cca3556.

[40] Ž. Jakopin, M. Gobec, I. Mlinarič-Raščan, M. Sollner Dolenc, Immunomodulatory Properties of Novel Nucleotide Oligomerization Domain 2 (Nod2) Agonistic Desmuramyldipeptides, J. Med. Chem. 55 (2012) 6478–6488. https://doi.org/10.1021/jm300503b.

[41] X. Wen, P. Zheng, Y. Ma, Y. Ou, W. Huang, S. Li, S. Liu, X. Zhang, Z. Wang, Q. Zhang, W. Cheng, R. Lin, H. Li, Y. Cai, C. Hu, N. Wu, L. Wan, T. Pan, J. Rao, X. Bei, W. Wu, J. Jin, J. Yan, G. Liu, Salutaxel, a Conjugate of Docetaxel and a Muramyl Dipeptide (MDP) Analogue, Acts as Multifunctional Prodrug That Inhibits Tumor Growth and Metastasis, J. Med. Chem. 61 (2018) 1519–1540. https://doi.org/10.1021/acs.jmedchem.7b01407.

[42] Y. Dong, S. Wang, C. Wang, Z. Li, Y. Ma, G. Liu, Antagonizing NOD2 Signaling with Conjugates of Paclitaxel and Muramyl Dipeptide Derivatives Sensitizes Paclitaxel Therapy and Significantly Prevents Tumor Metastasis, J. Med. Chem. 60 (2017) 1219–1224. https://doi.org/10.1021/acs.jmedchem.6b01704.

[43] X. Li, J. Yu, S. Xu, N. Wang, H. Yang, Z. Yan, G. Cheng, G. Liu, Chemical conjugation of muramyl dipeptide and paclitaxel to explore the combination of immunotherapy and chemotherapy for cancer, Glycoconj. J. 25 (2008) 415–425. https://doi.org/10.1007/s10719-007-9095-3.

[44] Y. Ma, N. Zhao, G. Liu, Conjugate (MTC-220) of Muramyl Dipeptide Analogue and Paclitaxel Prevents Both Tumor Growth and Metastasis in Mice, J. Med. Chem. 54 (2011) 2767–2777. https://doi.org/10.1021/jm101577z.

[45] M. Sollner, V. Kotnik, Pečar, A. Štalc, S. Simčič, L. Povšič, B. Herzog-Wraber, L. Klampfer, A. Ihan, P. Grosman, Apyrogenic synthetic desmuramyldipeptide, LK-409, with immunomodulatory properties, Agents Actions. 38 (1993) 273–280. https://doi.org/10.1007/BF01976220.

[46] M. Sollner, S. Pečar, A. Štalc, The influence of the lipophilicity of 7-oxoacyl-l-alanyl-d-isoglutamines on their immunorestoration activity in vivo, Eur. J. Med. Chem. 31 (1996) 927–933. https://doi.org/10.1016/S0223-5234(97)89858-3.

[47] M. Gobec, I. Mlinarič-Raščan, M.S. Dolenc, Ž. Jakopin, Structural requirements of acylated Gly- l -Ala- d -Glu analogs for activation of the innate immune receptor NOD2, Eur. J. Med. Chem. 116 (2016) 1–12. https://doi.org/10.1016/j.ejmech.2016.03.030.

[48] M. Moriguchi, K. Urabe, N. Norisada, C. Ochi, A. Stalc, U. Urleb, S. Muraoka, Therapeutic Effects of LK 423, a Phthalimido-desmuramyldipeptide Compound, on Dextran Sulfate Sodium-Induced Colitis in Rodents Through Restoring, Arzneimittelforschung. 49 (2011) 184–192. https://doi.org/10.1055/s-0031-1300400.

[49] C. Ochi, N. Norisada, M. Moriguchi, A. Stalc, U. Urleb, S. Muraoka, lnterleukin-10 Inducing Activity of LK423, a Phthalimido-desmuramyldipeptide Compound, Arzneimittelforschung. 49 (2011) 72–79. https://doi.org/10.1055/s-0031-1300363.

[50] Ž. Jakopin, E. Corsini, M. Gobec, I. Mlinarič-Raščan, M.S. Dolenc, Design, synthesis and biological evaluation of novel desmuramyldipeptide analogs, Eur. J. Med. Chem. 46 (2011) 3762–3777. https://doi.org/10.1016/j.ejmech.2011.05.042.

[51] K. Keček Plešec, D. Urbančič, M. Gobec, A. Pekošak, T. Tomašič, M. Anderluh, I. Mlinarič-

Raščan, Ž. Jakopin, Identification of indole scaffold-based dual inhibitors of NOD1 and NOD2, Bioorg. Med. Chem. 24 (2016) 5221–5234. https://doi.org/10.1016/j.bmc.2016.08.044.

[52] D.H.R. Barton, J. Camara, P. Dalko, S.D. Gero, B. Quiclet-Sire, P. Stuetz, Synthesis of biologically active carbocyclic analogs of N-acetylmuramyl-L-alanyl-D-isoglutamine (MDP), J. Org. Chem. 54 (1989) 3764–3766. https://doi.org/10.1021/jo00277a002.

[53] N. Inohara, Y. Ogura, A. Fontalba, O. Gutierrez, F. Pons, J. Crespo, K. Fukase, S. Inamura, S. Kusumoto, M. Hashimoto, S.J. Foster, A.P. Moran, J.L. Fernandez-Luna, G. Nuñez, Host Recognition of Bacterial Muramyl Dipeptide Mediated through NOD2, J. Biol. Chem. 278 (2003) 5509–5512. https://doi.org/10.1074/jbc.C200673200.

[54] A. Adam, E. Lederer, Muramyl peptides: Immunomodulators, sleep factors, and vitamins, Med. Res. Rev. 4 (1984) 111–152. https://doi.org/10.1002/med.2610040202.

[55] E.W. Ades, J.R. Schmidtke, Immunotherapy of Infectious Diseases, in: H.-J. Hess (Ed.), Annu. Reports Med. Chem. Vol. 18, Academic Press, Inc., New York, 1983: p. 153.

[56] J. Danklmaier, H. Honig, Synthesis of Acyclic Analogs of N-Acet ylmuramyl-L-alanyI-D-isoglutamine (MDP), Liebigs Ann. Chem. (1990) 145–150.

[57] F.-A. Khan, M. Ulanova, B. Bai, D. Yalamati, Z.-H. Jiang, Design, synthesis and immunological evaluation of novel amphiphilic desmuramyl peptides, Eur. J. Med. Chem. 141 (2017) 26–36. https://doi.org/10.1016/j.ejmech.2017.09.070.

[58] T.E. Klepach, I. Carmichael, A.S. Serianni, Geminal 2 J CCH Spin−Spin Coupling Constants as Probes of the φ Glycosidic Torsion Angle in Oligosaccharides, J. Am. Chem. Soc. 127 (2005) 9781–9793. https://doi.org/10.1021/ja040251y.

[59] P. Sizun, B. Perly, M. Level, P. Lefrancier, S. Fermandjian, Solution Conformations of the Immunomodulatory Muramyl Peptides, Tetrahedron. 44 (1988) 991–997.

[60] O. Takeuchi, S. Akira, Pattern Recognition Receptors and Inflammation, Cell. 140 (2010) 805–820. https://doi.org/10.1016/j.cell.2010.01.022.

[61] M. V. Pashenkov, N.E. Murugina, A.S. Budikhina, B. V. Pinegin, Synergistic interactions between NOD receptors and TLRs: Mechanisms and clinical implications, J. Leukoc. Biol. 105 (2019) 669–680. https://doi.org/10.1002/JLB.2RU0718-290R.

[62] M.A. Wolfert, T.F. Murray, G.-J. Boons, J.N. Moore, The Origin of the Synergistic Effect of Muramyl Dipeptide with Endotoxin and Peptidoglycan, J. Biol. Chem. 277 (2002) 39179–39186. https://doi.org/10.1074/jbc.M204885200.

[63] O. Gutierrez, C. Pipaon, N. Inohara, A. Fontalba, Y. Ogura, F. Prosper, G. Nunez, J.L. Fernandez-Luna, Induction of Nod2 in myelomonocytic and intestinal epithelial cells via nuclear factor-kappa B activation., J. Biol. Chem. 277 (2002) 41701–5. https://doi.org/10.1074/jbc.M206473200.

[64] M.D. Turner, B. Nedjai, T. Hurst, D.J. Pennington, Cytokines and chemokines: At the crossroads of cell signalling and inflammatory disease, Biochim. Biophys. Acta - Mol. Cell Res. 1843 (2014) 2563–2582. https://doi.org/10.1016/j.bbamcr.2014.05.014.

[65] A. Roychowdhury, M.A. Wolfert, G.-J. Boons, Synthesis and Proinflammatory Properties of Muramyl Tripeptides Containing Lysine and Diaminopimelic Acid Moieties, ChemBioChem. 6 (2005) 2088–2097. https://doi.org/10.1002/cbic.200500181.

[66] K. Dzierzbicka, A. Wardowska, M. Rogalska, P. Trzonkowski, New conjugates of muramyl

dipeptide and nor-muramyl dipeptide linked to tuftsin and retro-tuftsin derivatives significantly influence their biological activity., Pharmacol. Rep. 64 (2012) 217–23. http://www.ncbi.nlm.nih.gov/pubmed/22580539.

[67] B. Cai, J.S. Panek, S. Amar, Convergent Synthesis of Novel Muramyl Dipeptide Analogues: Inhibition of Porphyromonas gingivalis -Induced Pro-inflammatory Effects by High Doses of Muramyl Dipeptide, J. Med. Chem. 59 (2016) 6878–6890. https://doi.org/10.1021/acs.jmedchem.6b00681.

[68] S. Bienert, A. Waterhouse, T.A.P. de Beer, G. Tauriello, G. Studer, L. Bordoli, T. Schwede, The SWISS-MODEL Repository—new features and functionality, Nucleic Acids Res. 45 (2017) D313–D319. https://doi.org/10.1093/nar/gkw1132.

[69] S.F. Altschul, W. Gish, W. Miller, E.W. Myers, D.J. Lipman, Basic local alignment search tool, J. Mol. Biol. 215 (1990) 403–410. https://doi.org/10.1016/S0022-2836(05)80360-2.

[70] S. Maekawa, U. Ohto, T. Shibata, K. Miyake, T. Shimizu, Crystal structure of NOD2 and its implications in human disease, Nat. Commun. 7 (2016) 11813. https://doi.org/10.1038/ncomms11813.

[71] D. Eisenberg, R. Lüthy, J.U. Bowie, VERIFY3D: Assessment of protein models with three-dimensional profiles, in: 1997: pp. 396–404. https://doi.org/10.1016/S0076-6879(97)77022-8.

[72] "Molecular Operating Environment (MOE), 2013.08; Chemical Computing Group ULC, 1010 Sherbooke St. West, Suite #910, Montreal, QC, Canada, H3A 2R7, 2018.," in: n.d.

[73] T.A. Halgren, Merck molecular force field. I. Basis, form, scope, parameterization, and performance of MMFF94, J. Comput. Chem. 17 (1996) 490–519. https://doi.org/10.1002/(SICI)1096-987X(199604)17:5/6<490::AID-JCC1>3.0.CO;2-P.

[74] T. Tanabe, M. Chamaillard, Y. Ogura, L. Zhu, S. Qiu, J. Masumoto, P. Ghosh, A. Moran, M.M. Predergast, G. Tromp, C.J. Williams, N. Inohara, G. Núñez, Regulatory regions and critical residues of NOD2 involved in muramyl dipeptide recognition, EMBO J. 23 (2004) 1587–1597. https://doi.org/10.1038/sj.emboj.7600175.

Highlights

1. New type of desmuramyl peptides having hydrophilic aryl scaffolds were synthesized.
2. Their preparation involves an efficient 12 step synthesis strategy.
3. They can effectively modulate the inflammatory response of THP-1 cells.
4. High levels of TNF-α – a major proinflammatory cytokine – were released.
5. Molecular docking studies indicate strong binding to NOD2 receptor.

Declaration of interests

☒ The authors declare that they have no known competing financial interests or personal relationships that could have appeared to influence the work reported in this paper.

☐The authors declare the following financial interests/personal relationships which may be considered as potential competing interests: